

# Contact Binaries of the Galactic Disk: Comparison of the Baade's Window and Open Cluster Samples

SLAVEK M. RUCINSKI

Electronic-mail: [rucinski@cfht.hawaii.edu](mailto:rucinski@cfht.hawaii.edu)

Canada – France – Hawaii Telescope Co.

P.O. Box 1597, Kamuela, HI 96743

October 12, 2018

## ABSTRACT

The paper attempts to integrate the available data for contact binaries of the disk population in a deep galactic field and in old open clusters. The two basic data sets consist of 98 systems in the volume-limited 3 kpc sub-sample of contact binaries detected by the OGLE microlensing project toward Baade's Window (BW<sub>3</sub>) and of 63 members of 11 old open clusters (CL). Supplementary data on the intrinsically bright, but spatially rare, long-period binaries are provided by 238 systems in the BW sample to the distance of 5 kpc (BW<sub>5</sub>). The basic BW<sub>3</sub> sample and the CL sample are remarkably similar in the period, color, luminosity and variability-amplitude distributions, in spite of very different selections, for BW<sub>3</sub> – as a volume-limited sub-sample of all contact systems discovered by the OGLE project, and for CL – as a collection of contact systems discovered in open clusters which had been subject to searches differing in limiting magnitudes, cluster area coverage and photometric errors. The contact systems are found in the color interval  $0.3 < (B - V)_0 < 1.2$  where the turn-off points (TOP) of the considered clusters are located; however, they are not concentrated at the respective TOP locations but, once the TOP happens to fall in the above color interval, they can appear anywhere within it.

The luminosity function for the BW sample appears to be very similar in shape to that for the solar neighborhood main-sequence (MS) stars when corrections for the galactic disk structure are applied, implying a flat apparent frequency-of-occurrence distribution. In the accessible interval  $2.5 < M_V < 7.5$ , the frequency of contact binaries relative to MS stars equals about 1/130 for the exponential disk length scale  $h_R = 2.5$  kpc and about 1/100 for  $h_R = 3.5$  kpc. The high frequency cannot continue for  $M_V < 2.5$  as the predicted numbers of bright systems would then become inconsistent with the numbers of known systems to  $V_{lim} = 7.5$  in the sky sample. The previous estimate of the frequency from the BW sample of 1/250 – 1/300 did not correctly relate the numbers of the contact binaries to the numbers of MS stars. The magnitude limit of the OGLE survey limits the accuracy of the current luminosity function determination for  $M_V > 5.5$ , but the available data are consistent with a

continuation of the high apparent frequency beyond  $M_V = 7.5$ , i.e. past the current short-period, low-luminosity end, delineated by the shortest-period field system CC Com at  $M_V = 6.7$ . The current data indicate that the sky-field sample starts showing discovery-selection effects at a level as high as  $V \simeq 10 - 11$ .

*Subject headings:* binaries: general – binaries: eclipsing – stars: statistics

## 1. INTRODUCTION

Contact stars are close binary systems in which components form single entities described by equipotentials of the Roche geometry. The most common among them consist of solar-type stars and are called W UMa-type binaries; their orbital periods are in the range between about one quarter and three quarters of a day. Several reviews have discussed properties of contact binaries; the recent ones, concentrating respectively on theoretical and observational issues have been by Eggleton (1996) and by Rucinski (1993). How these binaries form and evolve is still poorly understood, but it is generally assumed that they are in the penultimate – but possibly long lasting – stage of angular-momentum-loss driven evolution, just before forming single stars. The angular-momentum-loss results from the torque exerted by the magnetized stellar wind on the components, which extracts the angular momentum from the orbit via the tidal synchronism of rotation. Since this process takes relatively long time, of the order of a few Gyrs for solar-type stars, the W UMa-type systems are expected to consist of relatively old stars. The evidence for their advanced age cannot be inferred from spectral signatures of low metal abundance because of the extremely strong broadening of spectral lines, but comes from (1) their relatively large spatial velocities (Guinan & Bradstreet 1988), characteristic for old disk stars, and their presence in (2) old open clusters (Kałużny & Rucinski 1993 = KR93, Rucinski & Kałużny 1994 = RK94) and in (3) the disk component toward Baade’s Window (Rucinski 1997a, see below).

For a long time, the statistics of contact binaries was particularly uncertain because of the accidental nature of the sky-field discoveries. One of the indications of incompleteness in the cataloged sky-field sample was the tendency to show only relatively large light-curve amplitudes whereas simple considerations of randomly distributed orbital inclinations suggest that low amplitude systems should be most common. Indeed, systematic searches in open clusters (KR93, RK94), later supplemented by the OGLE microlensing by-product data (Rucinski 1997a = R97a, Rucinski 1997b = R97b; see below), led to the discovery of many low amplitude systems. The cluster searches also permitted to address the question of the ages. A progression in numbers of such systems with the cluster age, in the sense of more systems in older clusters, supported the view that the contact systems form over time from close, detached binary systems. The initial interpretations of the old open cluster data (KR93, RK94) indicated the apparent<sup>1</sup> frequency in

---

<sup>1</sup>Unless specifically noted, the frequency of occurrence of contact systems discussed in this paper is *apparent*, i.e.

clusters by an order of magnitude higher than had been estimated for the sky field (Duerbeck 1984), reaching perhaps one such a system per hundred main sequence stars. When projected non-members were removed from clusters at low galactic latitudes and data for several clusters were averaged to improve the number statistics, the apparent frequency relative to the number of monitored MS stars of spectral types F to K was estimated to be about one such a system per 250 – 300 ordinary stars (Rucinski 1994 = CAL1). Although these numbers were approximate, they indicated that in a typical old open cluster, where some thousand or so stars could be monitored for variability, only a few contact systems would be normally found, a circumstance making any meaningful statistical inferences difficult. Thus, the cluster data could not offer sound statistics and larger, more uniform data sets were needed.

Very recently, massive discoveries of contact systems in microlensing surveys offered an abundant source of statistical data. Two thirds among 933 eclipsing binaries discovered in the OGLE-1 survey (R97a, R97b) have been classified as contact binaries. While the discoveries yielded unprecedented material for studies of contact binaries in various ways (R97a, R97b, Rucinski 1998 = R98), one aspect has been of particular importance in the present context: The OGLE data permitted to define a volume-limited sample of contact binaries, leading to the first unbiased estimates of frequency distributions for such parameters as orbital periods, colors or luminosities. The contact systems were found to appear in unexpectedly narrow ranges of periods, mainly within  $0.25 < P < 0.7$  day, and colors,  $0.2 < (V - I)_0 < 1.5$  (several observational effects could make the observed color range slightly broader than in reality, see Section 4). The range in colors – coinciding with location on the color–magnitude diagrams where solar-type, old-disk stars start showing evolutionary effects – led to a suggestion (R97a) that the properties of these systems have an evolutionary relation to the Turn-Off Point (TOP) stage of evolution, when the components expand and enter into physical contact. This suggestion is testable since the cluster data of the CL sample permit to relate positions of contact systems and TOP’s in color–magnitude diagrams.

This paper discusses properties of contact binaries toward Baade’s Window (BW) and in old open clusters (CL), to uncover similarities and differences in the two sets of data. The two samples are complementary, as the BW sample contains objects observed in a uniform fashion, but with absolute magnitudes and implied distances determined through one particular calibration, while the CL sample consist of objects with independent information on age, metallicity and distance, but from an group of clusters which were selected in a somewhat non-rigorous fashion. This paper utilizes also a new, very useful tool which had not been available before, the new  $M_V = M_V(\log P, B - V)$  calibration which is based on the Hipparcos parallaxes (Rucinski & Duerbeck 1997 = CAL5). The calibration obviates any needs to resort to absolute magnitude

---

it is not corrected for missed systems with low orbital inclination angles. It is expected that the correction factor is of the order of 1.5 to 2.0, but it cannot be predicted a priori as its value crucially depends on the mass-ratio distribution, which is unknown, see R97b. In the same sense, when we discuss “complete” samples later on, we mean samples of those systems which are discoverable for a given minimum amplitude threshold.

calibrations based on open clusters, whose use could imply an obvious risk of a circular reasoning. We stress that this paper utilizes the Hipparcos-based *calibration*, but does not utilize the Hipparcos *sample* of the contact binaries in the solar vicinity. The reason is the biased character of the Hipparcos sample which, being magnitude-limited, consists primarily of intrinsically luminous systems. We note, that the Hipparcos observed all stars of the sky only to slightly beyond  $V \simeq 7$  and only six contact binaries actually exist to this magnitude limit.

The paper is organized as follows: Section 2 describes the BW and CL samples. The next sections compare various properties and statistics for the two samples: the period (Section 3) and color (Section 4) distributions, the color – magnitude diagrams (Section 5), the period – color relations (Section 6) and the variability amplitudes (Section 7). The important matter of the frequency of occurrence of the contact systems is addressed in Section 9, after a discussion of the related issue of the luminosity functions in Section 8. The last Section 10 contains conclusions of the paper.

## 2. THE TWO SAMPLES

### 2.1. The Baade’s Window sample (BW)

The volume-limited BW sample has been defined in R97a. It consists of 98 systems with orbital periods shorter than one day and distances smaller than 3 kpc, which passed the Fourier light-curve shape filter. Comparison of the number densities for the volumes defined by the distances of 2 kpc and 3 kpc indicated that the 3 kpc sample is complete to its limiting absolute magnitude of  $M_I = 4.5$ , which – for typical values of reddening and intrinsic colors – translates into an approximate limit of  $M_V \simeq 5.5$ . Among the BW-sample systems, most are genuine W UMa-type systems with approximately equally-deep eclipses, indicating perfect thermal contact between components. However, two systems did pass the light-curve shape filter used to select contact systems, yet had eclipse depth differences large enough to suspect poor thermal contact, or more likely, very close semi-detached configurations; the accompanying asymmetries of the maxima suggest in such cases an on-going mass transfer (R97b). Thus two, among 98 systems, i.e. only about 2 percent of all contact systems appear to be of this type, although – by being intrinsically more luminous than typical W UMa-type systems due to longer periods – they are much more common in the sky-field (or any other magnitude-limited) sample. For simplicity, we will call them Poor Thermal Contact (PTC) systems, remembering that these could be either contact systems with inhibited energy transfer or very close semi-detached binaries.

The intrinsically bright, long-period systems can be observed deeper in space. By selecting a deeper sample, we can analyze the long-period and high-luminosity ends of the respective distributions, sacrificing the statistics at the faint, short period end. For that purpose, a second BW sample to 5 kpc has been considered in this paper. It is based on a 4.6 times larger volume than the 3 kpc sample and contains 238 system, 8 of them showing the PTC light curves. Its

statistical properties are sound only for systems with periods longer than about 0.55 day as the short-period ones are eliminated by their low absolute magnitudes (see Figure 13 in R97a). The expected completeness limit of the 5 kpc BW sample is  $M_V \simeq 4.2$  (thus the  $3.5 < M_V < 4.5$  bin is partly affected in various statistics presented later). Whenever relevant, we will distinguish the two Baade’s Window sub-samples by subscripts, BW<sub>3</sub> and BW<sub>5</sub>, but normally, for most considerations, the basic sample BW<sub>3</sub> will be used.

Only one system with a period longer than one day, BW5.009 with  $P = 1.59$  day, from the sample discussed in R98 could be formally included in the BW<sub>5</sub> sample (its distance is about 4.3 kpc). However, its luminosity and distance are poorly known due to lack of the luminosity calibration for very blue contact systems (the observed  $V - I = 1.01$  and the estimated  $E_{V-I} = 0.84$ ). This system is disregarded in the current paper.

The original data in the OGLE catalog consist of the maximum brightness  $I$  and  $V - I$  magnitudes and colors, orbital periods  $P$ , amplitudes in  $I$  and coordinate positions. The analysis presented in R97a and R97b added to these data the light-curve-decomposition Fourier coefficients as well as the distances, absolute magnitudes  $M_I$  and reddening corrections  $E_{V-I}$ . These data for all contact binaries in the OGLE survey are available in the form of extensive tables via Internet at: <http://www.cfht.hawaii.edu/~rucinski/rucinski.html> (the major tables of this paper are also in this location). Since our basic 3 kpc volume-limited sample has not yet been published, but may have a more general use, we present it in Table 1. The table contains the original data from OGLE as well as the derived quantities in the  $V$ ,  $B - V$  photometric system. The transformation of the photometric data, rather than the use of the original  $I$ ,  $V - I$  data (which would have many advantages because of usually higher accuracy and weaker sensitivity of that color to entirely unknown metallicities), has been mandated by the fact that most open clusters were observed in the  $V$ ,  $B - V$  system, and that the Hipparcos calibration is available only in this system. The transformations were:  $M_V = M_I + (V - I) - E_{V-I}$  for the absolute magnitudes; the reddening-corrected colors  $(V - I)_0$  have been transformed into  $(B - V)_0$  with the main-sequence relations of Bessell (1979, 1990).

## 2.2. The cluster sample (CL)

The open cluster sample (CL) has been obtained by combining the data published in several papers, most of them by Kałuzny and collaborators. The assumed cluster properties are listed in Table 2 which is arranged in the age progression, from the oldest to the youngest clusters. To obtain the best uniformity of the material, the values of reddening corrections  $E_{B-V}$  and apparent distance moduli,  $(m - M)_V$ , were taken from the recent tabulation of Twarog et al. (1997). The ages have been taken mostly from the original publications, and then adjusted slightly for consistency of the color-magnitude diagrams (Section 5). The ages are only approximate and used here mainly to arrange the clusters into an age progression. References to the sources of the photometric data are given in the last column of Table 2.

Table 3 lists the data for the contact systems detected in the cluster fields. The systems are ordered by the new variable-star designations, following the 71st, 72nd and 73rd Variable-Star Name lists (Kazarovets et al. 1993, Kazarovets & Samus 1995, 1997). Since these designations are used for the first time for many of the listed systems, the original names in the discovery papers are also given. Most of the photometric data are available in the  $V$ ,  $B - V$  system. For those clusters which were observed in the  $V - I$  system and for those with both colors available, the main-sequence color-color transformations to  $B - V$  were used, as the  $V - I$  data were usually of better quality than those in  $B - V$ .

The Fourier light-curve shape filter was not applied to the CL systems to verify their W UMa-type characteristics. The main reason was the partial phase coverage for many systems which frequently resulted in erroneous values of the Fourier coefficients and rejection of otherwise apparently genuine cluster members. For this reason, the CL sample may contain a small admixture of other short-period variable stars; in this sense, the internal consistency of the CL sample is poorer than that of the BW sample. The cluster membership was verified using the absolute-magnitude Hipparcos calibration CAL5:  $M_V^{cal} = -4.44 \log P + 3.02 (B - V)_0 + 0.12$ , where  $(B - V)_0 = (B - V) - E_{B-V}$ . The absolute magnitudes listed in Table 3 have been obtained using the observed maximum-light magnitudes,  $V_{max}$ , and the cluster distance moduli,  $(m - M)_V$ :  $M_V = V_{max} - (m - M)_V$ . Large deviations  $\Delta M_V = M_V - M_V^{cal}$  permitted to identify systems located in front or behind the respective clusters. The deviations form a distribution which shows long tails of non-members on both sides of the maximum, but which within  $-2 < \Delta M_V < +2$  can be rather well described by a Gaussian with the dispersion  $\sigma = 0.47$  and with the mean at  $-0.04$ . The small shift in the mean value is gratifying as it shows that the Hipparcos and cluster samples are mutually consistent. However, the dispersion of  $\Delta M_V$  is large when compared with that for the Hipparcos sample which showed an intrinsic scatter of  $\sigma_{HIP} = 0.22$ . We suspect that a large fraction of the scatter comes from the uncertainties in the cluster data. This is indicated by systematically smaller deviations for some better observed clusters such as M 67. But notice also that some apparently genuine cluster members (such as ER Cep in NGC 188) in well-observed clusters do show large deviations. For some clusters, the deviations may have been increased because no account was made for differing, but usually poorly known metallicities (as in the case of Tom 2). Instead of inventing a system of weights for individual clusters, it was decided simply to widen the range for the membership acceptance in  $\Delta M_V$  to  $\pm 1.0$ , that is to  $\pm 2.1\sigma$  of the  $\Delta M_V$  distribution. While this way some non-members may have entered to spoil our statistics, we note that the application of the Hipparcos calibration resulted – in most cases – in smaller deviations in  $M_V$  than in the discovery papers where individual membership criteria were first discussed. Thus, many systems which would not pass the  $\pm 1$  magnitude deviation filter on the basis of the older calibrations CAL1 and CAL2 (Rucinski 1994, 1995) can now be considered as cluster members.

In two cases, V514 Lyr (NGC 6791–V8) and IK CMa (Be 33–V2), the deviations are slightly larger than the adopted threshold; in both cases  $\Delta M_V = -1.05$ . An inconsistency has been committed here by removing V514 Lyr from the CL sample, but retaining IK CMa. The basic

photometric data for NGC 6791 are sufficiently well known to verify that the membership of V514 Lyr to the cluster is quite unlikely. In contrast, the large and poorly known reddening ( $E_{B-V} \simeq 0.7$ ) and, possibly, the low metallicity of Be 33 leave a large margin of uncertainty in the cluster properties to retain IK CMa as a probable member. This is the only system in Be 33 which can be considered as a member (the other one, II CMa = Be 33–V1 is definitely not). Be 33 is the youngest of the clusters in the sample, so that it is easy to keep IK CMa apart and see if it deviates in any other sense. As far as we can see, the system belongs to this cluster.

The cluster surveys for variability have different depth and reach different levels of absolute magnitudes. An attempt has been made to estimate roughly the levels at which detection of variability would become impossible because of the rapid increase of errors for fainter stars. These limiting levels,  $M_V^{lim}$ , were estimated on the basis the cluster distance moduli and the photometric-error data given in most of the papers by Kałużny and collaborators as the points where the errors reached about 0.05 mag.; for such errors, variables with amplitudes of about 0.1 mag should be still detectable. The limiting  $M_V^{lim}$  are given in Table 2 and shown later in the color – magnitude diagrams shown in Section 5. Typically, the nominal depths are  $M_V^{lim} \simeq 6 - 7$ , with the exception of the distant and photometrically difficult clusters Tom 2 and Be 33, where the limits are at the level of about  $M_V \simeq 5$ . It should be stressed that these limits are approximate and somewhat subjective so that the CL sample is much less rigorously defined, especially at its faint end, than the BW sample.

In forming the CL sample, no account has been made of the fact that some searches of open clusters gave no discoveries of contact systems. The number of failed searches is not known. Only one case has been published of such a failed search in 6 clusters (NGC 2360, 2420, 2506, 6802, 6819 and Mel 66) by Kałużny & Shara (1988); in one of these clusters, NGC 6802, a very low amplitude W UMa system was subsequently found (Vidal & Belmonte 1993). We have no explanation for the lack of contact systems in some clusters and we do not know if this is a real phenomenon or some statistical or observational effect. Whatever is the cause, it clearly shows the limitations of the CL sample which is less rigorously defined than the BW<sub>3</sub> sample.

### 3. PERIOD DISTRIBUTION

A comparison of the BW and CL samples is shown in Figure 1. Since we have 98 objects of the BW<sub>3</sub> sample and 63 objects of the CL sample, this figure and the following similar ones have the left and right side vertical scales scaled in proportion of 3:2 to take into account approximately the difference in sizes of the two samples. The histograms in Figure 1 and in the following similar figures are not normalized in order to show the numbers of the W UMa-type systems in each bin and thus permit a direct judgment on the Poisson uncertainties involved. We can see that whatever statistical properties we would like to analyze in this paper, the results will be relevant to the most common contact binaries only; objects appearing at frequencies lower than a few percent of the totality are expected to be missed. The BW<sub>5</sub> sample consisting of 238 objects has

been added to improve the statistics for the intrinsically rare, but bright, long-period systems which can be seen to large distances.

Taking into account the large per-bin uncertainties in the histograms, the period distributions for the BW<sub>3</sub> and CL samples (Figure 1) are surprisingly similar, especially when plotted in linear units of the orbital period (the left panel in the figure). Both samples show sharp cutoffs at the orbital periods of about 0.22 – 0.25 day, and maxima at about 0.35 – 0.4 day. Systems with periods longer than about 0.7 day are absent in BW<sub>3</sub> but do appear in BW<sub>5</sub> at the level of about 0.5 percent of all systems. The short period cutoffs are located at 0.228 day, defined by BW4.040<sup>2</sup>, and 0.225 day, defined by V702 Mon in Be 39; both are very close to the current record of 0.221 day for the field system CC Com (Rucinski 1977). Application of the two-distribution Kolmogorov – Smirnov test gives only 0.6 percent significance to the hypothesis that the BW and CL distributions are different, when binned in linear units of the orbital period. The same significance with the logarithmic binning is 3.5 percent.

The period distribution for the BW<sub>5</sub> sample indicates that contact systems with periods longer than 0.7 day are very rare, but not absent, as could be perhaps erroneously inferred from the BW<sub>3</sub> sample. They become detectable when sufficiently large volume is searched. While Figure 1 shows the numbers for BW<sub>5</sub> simply scaled by 5 relative to BW<sub>3</sub>, to allow for the difference in the search volumes in an approximate way, Figure 2 and Table 4 give the exact relation in the form of what we call the *period function*, PF. It is an analogue of the luminosity function and gives the number of contact binaries in constant intervals of  $\log P$  per unit of volume. The respective volumes of the samples to the distances of 3 kpc and 5 kpc used to derive these functions were  $1.22 \times 10^6 \text{ pc}^3$  and  $5.64 \times 10^6 \text{ pc}^3$ . Errors of the PF's can be obtained by scaling by the  $1/\sqrt{N}$ , where  $N$  are the numbers of systems in the respective period bins. The period function derived from BW<sub>5</sub> can be used only above  $P \simeq 0.55$  day (or  $\log P \simeq -0.25$ ) because distant, short-period, low-luminosity systems are eliminated from it by the magnitude limit of the OGLE survey at  $I = 17.9$ . The entries of PF<sub>5</sub> which are affected by this selection effect are taken in Table 4 in square brackets. The period function are based on the apparent numbers of systems and are not corrected for the systems missed because of the low orbital inclination angles.

#### 4. COLOR DISTRIBUTION

The color distribution for the BW<sub>3</sub> sample in the  $I, V - I$  system was discussed in R97a. For comparison of the BW<sub>3</sub> and CL samples, the BW<sub>3</sub> data have been transformed here to the  $B - V$  color index. The BW<sub>5</sub> sample is not used in the comparison because its color distribution is affected by elimination of faint, red systems. Figure 3 shows a comparison of histograms

---

<sup>2</sup>We use the same convention as in R97a in that the first digit gives the OGLE field, and the number of the variable in the field is given after the period.



representing the distributions for BW<sub>3</sub> and CL. The agreement is not as close as in the case of the period distributions. The two-distribution K–S test gives a 30 percent significance for rejection of the null hypothesis of identical distributions. The difference in the distributions is caused mostly by the spike in the CL distribution at  $(B - V)_0 = 0.75$ . However, the end points of the color distributions coincide well, with the distribution for BW<sub>3</sub> being a bit wider – as expected – because of the reddening correction uncertainties. In fact, four observational effects are expected to broaden the BW<sub>3</sub> color distribution; these are: (1) uncertainties in the reddening in Baade’s Window, mostly from the spotty character of the reddening, (2) the crude model of the reddening adopted in R97a, (3) photometric blending of stars in the extremely dense BW field and (4) the  $(V - I)_0$  to  $(B - V)_0$  color transformations.

Because the BW<sub>3</sub> sample is expected to be complete and statistically better defined than the CL sample, we will tolerate the possibly larger color uncertainties for the BW<sub>3</sub> systems and use this sample in the next Section 5 as an external reference for comparison with individual clusters. The total range of colors observed for the BW<sub>3</sub> sample is  $0.19 < (B - V)_0 < 1.54$ . Because of the possibility of errors for individual systems, we will also consider the 90 percent range, here defined as the interval where 90 from among 98 systems of the BW<sub>3</sub> sample are located. This range extends over  $0.3 < (B - V)_0 < 1.2$  and almost perfectly coincides with the full range observed for all binaries of the CL sample, which extends over  $0.31 < (B - V)_0 < 1.21$ . We note that while relatively red systems are seen in the BW<sub>3</sub> sample, none of the stars in the CL sample is as red as CC Com with  $(B - V)_0 = 1.24$  (Rucinski 1977); this is partly expected as  $M_V = 6.7$  of CC Com is close to, or perhaps even beyond the limiting levels of the cluster searches.

## 5. COLOR – MAGNITUDE DIAGRAMS

The color – magnitude diagram for the BW<sub>3</sub> sample is shown in Figure 4. The thin lines in the figure give the observed isochrones for Praesepe and NGC 6791, which are used for reference. The former is a moderately old cluster with age about 0.9 Gyr while the latter is one of the oldest clusters known with age of about 6 – 8 Gyr. Only one cluster in the CL sample is younger than Praesepe. It is Be 33, at 0.7 Gyr. However, as was commented in Section 2, we are not sure if its only member, IK Lyr, really belongs to it so it has been decided to use Praesepe as a case of a “young” old open cluster with a contact system.

The band of the contact systems in Baade’s Window in Figure 4 extends along the main sequence with a width of about 1 magnitude, and shows a concentration of systems in the region of the TOP of the oldest galactic disk population. The width of the sequence may be due to observational errors and spots on the stars, but also to a spread in the mass-ratios. The latter is entirely unaccounted in the absolute magnitude calibration, but its influence can be predicted by considering how total luminosity and total radiating area change with variation in the mass ratio. A small insert in the lower left corner illustrates how changes in the mass-ratio can modify the position of a contact system in the color–magnitude diagram (for details, see CAL5). For identical

stars ( $q = 1$ ), the shift is upward by  $-0.75$  mag, but for less massive secondary components ( $q \rightarrow 0$ ), the secondaries provide always relatively more radiating area than luminosity, so that the color becomes redder. The color shift is the largest for moderate mass-ratios around  $q \simeq 0.5 - 0.6$ .

Figures 5 – 7 show the positions of contact systems in the individual clusters. For each cluster, the approximate run of the respective observed isochrone is shown, together with positions of the isochrones for Praesepe and NGC 6791. Close examination of the figures shows that the contact systems are *not* concentrated in the immediate vicinity of the respective TOP’s. In fact, in those clusters where many systems were detected, such as Cr 261 or Be 39, the systems appear on both sides of each TOP, among the MS systems as well as among the Blue Stragglers. In all cases, except (marginally) for Praesepe and for Be 33 (where the association of the only system to the cluster may be questioned), the locations of the TOP’s themselves fall within the 90 percent range of the BW<sub>3</sub> sample, that is  $0.3 < (B - V)_0 < 1.2$ . What we see is not that the positions of the systems are related to the location of the TOP, but rather, that once the cluster TOP falls into the above range, the systems can then appear anywhere within it. Compare, for example, the diagrams for populous clusters such as Cr 261, Be 39 or M 67. In the last case, only 3 systems are known, but they span the whole width of the color range.

The last panel of Figure 7 contains the main sequence of Praesepe with superimposed marks giving masses according to a  $M_V$ -mass calibration for disk stars by Kroupa et al. (1993). As was discussed above, and as the inserts in the figures illustrate, the unknown mass-ratios can modify the luminosities and colors to some extent, but we can expect that these would be the primary components which would define positions of the systems in the color-magnitude diagrams. Thus, the last panel of Figure 7 gives a rough idea about the primary-component masses involved. They are apparently concentrated in the range of about  $0.65 - 1.6 M_\odot$ , with the maximum close to the  $1 M_\odot$ . Thus, as has been known for some time, the contact binaries of the W UMa-type are typically composed of solar-type stars.

## 6. PERIOD – COLOR RELATION

The period-color (PC) relation is a useful tool for studies of contact binaries. Effectively, it is a relation similar to the color-magnitude diagram, but with one of the photometric parameters replaced by the orbital period, which is known with an accuracy several orders of magnitude higher than either brightness or color. The PC relation for the BW<sub>3</sub> sample (with  $V - I$  as the base color) was presented in R97a, where the special significance of the short-period blue-envelope (SPBE) was also stressed. The concept of the SPBE is similar to that of the Zero-Age main sequence, in the sense that a system can move only in certain directions away from the SPBE. Here, in the period – color plane, the directions are down and right (see Figure 8). A system can be redder and larger (i.e. can have a longer orbital period) because of the evolutionary effects, while its color can be also redder because of the interstellar reddening. Location of the SPBE does depend on metallicity, and for low  $[\text{Fe}/\text{H}]$  it is shifted to bluer colors and shorter periods (CAL2).

The PC relation for the BW<sub>3</sub> sample using the  $(B - V)_0$  color is shown in Figure 8. A new fitting formula for the SPBE which is over-plotted in the figure was found by matching the previously used expression,  $(V - I)_{SPBE} = 0.053 \times P^{-2.1}$ , after its transformation into  $B - V$  using the MS transformations of Bessell (1979, 1990). It is:  $(B - V)_{SPBE} = 0.04 \times P^{-2.25}$ . It must be stressed that the numerical values in both formulae have no physical significance. A few systems located slightly above the SPBE may be low-metallicity objects or cases of poor/blended photometry. What is unusual in Figure 8 is that we do not see a well-defined *period-color relation*, because the scatter is large, primarily due to the presence of some red, long-period systems filling the lower right of the figure. While their locations are not a priori impossible, we do not see such systems in the sky-field sample (eg. the Hipparcos sample, CAL5), or in the CL sample (see Figure 9). We suspect that photometric blending of images leading to wrong colors or wrong reddening corrections and/or period aliases may have resulted in populating this part of the PC diagram. Inspection of the OGLE light-curve data indicates that only two systems in this region have well defined light curves, whereas most of the curves show small amplitudes and a large photometric scatter, which is possibly due to the use of period aliases<sup>3</sup>.

Because the SPBE is not expected to differ much within the range of metallicities observed for the clusters of the CL sample, all cluster systems are included in Figure 9. They have been divided into two groups to avoid congestion of the symbols. The four oldest, most populous clusters are shown in the upper panel of the figure, while the younger ones are collected in the lower panel. We see signatures of low metallicity for the systems in Tom 2 and Be 33, but the rest conform to the expected tendency of confinement below the SPBE for normal-metallicity contact systems. Open symbols signify Poor Thermal Contact systems. Two among them, one in Cr 261 and one in NGC 188, are clearly more evolved, showing longer orbital periods than systems of similar colors.

## 7. AMPLITUDES OF LIGHT VARIATIONS

As was discussed in Section 5 of R97b, distributions of the light-curve amplitudes contain information about the mass-ratio distribution. Because the light curves are dominated by geometrical effects of the strong distortion of the components, rather than by properties of stellar atmospheres (such as limb and gravity darkening laws), it is relatively easy to predict distributions of the amplitudes of light variations assuming random orbital inclinations and some plausible mass-ratio distributions. When mass-ratios are large ( $q \rightarrow 1$ ), large and small amplitudes can be observed, depending on the orbital inclination, but when the mass-ratios are small, only small amplitudes are possible, irrespectively of the inclination. However, the inverse problem of *determination* of the mass-ratio distribution,  $Q(q)$ , from the amplitude distribution,  $A(a)$ , is not

---

<sup>3</sup>The systems with good light curves, but then possibly wrong colors, are BW3.053 and 7.147, while the low amplitude systems showing large light-curve scatter are: BW3.022, 3.053, 5.075, 5.143, 5.157, 6.123, 7.112. Note that 3.053 and 7.112 are also among systems appearing in the faint tail in the  $M_V$  distribution in Figure 11.

an easy one as it would involve a solution of an integral equation representing a convolution of distributions (R97b). Such a determination could be contemplated for a sample of the order of one thousand objects or more.

Here, we limit ourselves to a comparison of the amplitude distributions for the BW<sub>3</sub> and CL samples which is shown in Figure 10. The distributions are apparently slightly different in that the CL sample appears to contain more large-amplitude systems than the BW<sub>3</sub> sample. The numbers per bin are small so the differences are not really significant. Besides, the difference can be explained by the use of the *I*-band amplitudes for the BW<sub>3</sub> sample which are expected to be systematically slightly smaller than the amplitudes in the *V* band. A simple scaling would not be prudent as conversions depend on combinations of geometrical parameters, but the effect is not expected to be larger than 3 to 8 percent. Thus, taking into account the per-bin uncertainties, we conclude that the amplitude distributions for the BW<sub>3</sub> and CL samples have basically identical shapes. However, as can be seen in Figure 10, both distributions are very different from that for the bright systems of the sky field (R97b), the latter being heavily biased by the large-amplitude systems which tended to be preferentially detected in non-systematic searches of the sky.

In the paper on Cr 261, Mazur et al. (1995) pointed out an interesting property of those contact systems which occur among the blue stragglers of the cluster: All of them were found to have small amplitudes, which raises a possibility that all of these systems have small mass-ratios. A meaningful analysis of the above effect could be done only for those clusters which have contact systems on both sides of the TOP. The amplitudes have been shown schematically for the clusters of the CL sample in Figures 5 – 7. There exist some differences between individual clusters, eg. in NGC 6791, all systems have small amplitudes, while all in NGC 188 have large amplitudes, but these may be due to small number statistics. Generally, we do not see any clear tendency for small amplitudes above the respective TOP's and Cr 261 remains the only cluster where the effect is rather clearly visible (the two PTC systems excepted). The tendency is not so obvious in Be 39 which is the next cluster in terms of the number of contact systems. As expected, the BW<sub>3</sub> sample does not show any segregation in the amplitudes along the main sequence, but this can be explained by a mixture of ages in the BW<sub>3</sub> sample. The amplitudes for that sample have been shown symbolically in Figure 4.

## 8. LUMINOSITY FUNCTION

The absolute magnitudes  $M_V$  for the BW and CL samples come from two entirely different determinations. The ones for the BW sample have been estimated via the  $M_I = M_I(\log P, (V - I)_0)$  calibration in R97a (this involved an iteration in  $E_{V-I}$ ), and then adjusted via  $M_V = M_I + (V - I)_0$ ; the ones for the CL sample result from the observed magnitudes  $V$  and assumed distance moduli of the clusters. In spite of coming from very different sources, the  $M_V$  absolute magnitude distributions turn out to be again similar, as can be seen in Figure 11, in that both show maxima in the interval  $3 < M_V < 6$ . The CL sample shows some deficiency at the faint end

relative to BW<sub>3</sub>, but is remarkably similar to BW<sub>5</sub> which we know to be more affected by the magnitude limit of the OGLE survey than BW<sub>3</sub>. For the limiting magnitude of the OGLE search of  $I_{lim} = 17.9$ , taking into account the interstellar extinction and the typical colors, as they vary along the absolute-magnitude sequence, the expected limits for BW<sub>3</sub> and BW<sub>5</sub> are  $M_V \simeq 5.5$  and  $M_V \simeq 4.2$ , respectively. Nominally, the CL sample should for some of the clusters reach depths of  $M_V \simeq 6 - 7$ , that is even deeper than the BW<sub>3</sub> sample; however, its low luminosity limit is, by necessity, a rather fuzzy one, being defined by the increases in the photometric errors for the contributing clusters rather than by a fixed distance, as in the case of the BW samples. Because of this deficiency, the CL sample is not considered in the discussion of the luminosity function. We have a good reasons to think that the BW<sub>3</sub> sample is fully complete to  $M_V \simeq 5.5$ , as the star number densities estimated to 3 kpc were found in R97a to be identical to those for 2 kpc. A few faint systems that populate the very tail of the BW distribution in Figure 11 to  $M_V \simeq 9$  must be nearby objects. They have been checked in the OGLE data for anomalies, but appear to have well defined light curves (but errors in colors are obviously possible); these are the variables BW3.053, 4.040 5.114, 7.112, 8.072. All of them, except BW7.112, have well defined light curve with large amplitudes.

The absolute magnitude distributions shown in Figure 11 have been converted into the luminosity functions (LF's) by simply dividing the system numbers by the total volumes of the BW<sub>3</sub> and BW<sub>5</sub> samples,  $1.22 \times 10^6 \text{ pc}^3$  and  $5.64 \times 10^6 \text{ pc}^3$ , for the depths of 3 kpc and 5 kpc, and for the  $40' \times 40'$  field of view. The limiting absolute magnitudes for the BW<sub>3</sub> and BW<sub>5</sub> samples (assuming constant interstellar absorption beyond 2 kpc, see R97a) are  $M_V = 5.5$  and 4.2, respectively. Beyond these completeness limits, the numbers of stars are expected to decrease because of the shrinking search volumes. These decreases should follow the standard 4-times per magnitude volume-size relation and thus can be accounted for by the volume corrections. Obviously, an application of such corrections magnifies the increasing Poisson errors so that an extension to fainter magnitudes can be done only slightly beyond the completeness limits of the survey. In our case, this extension was made into only two or three bins beyond the respective completeness limits of the BW samples.

The luminosity functions derived for the total volumes of the BW<sub>3</sub> and BW<sub>5</sub> samples are listed in Table 5. In this table,  $N_3$  and  $N_5$  are the numbers of contact systems in the BW<sub>3</sub> and BW<sub>5</sub> samples in one magnitude wide bins, centered on  $M_V$ .  $LF_3^{obs}$  and  $LF_5^{obs}$  are the corresponding observed luminosity functions, in units of  $10^{-5} \text{ pc}^{-3}$ , with entries which have been corrected by the volume correction of 3.981 times per one magnitude increment taken in square brackets.

In addition to the observed luminosity functions for the BW<sub>3</sub> and BW<sub>5</sub> samples, Figure 12 shows the luminosity function for the solar neighborhood MS stars  $LF_{MS}$  (Wielen et al. 1983), which has been arbitrarily scaled down by a factor of 130. This factor was selected to approximately match both  $LF_{BW}^{obs}$  in the interval  $3 < M_V < 5$  where the statistics should be the most reliable, i.e. it should not be affected by small-number fluctuations at the bright side and discovery-selection effects at the faint side. Obviously, the same factor of 130 gives the inverse apparent frequency for

the W UMa-type systems and directly shows that these binaries are indeed very common. We discuss the frequency of occurrence more fully in the next section.

A comparison of the luminosity functions in Figure 12 reveals surprisingly close similarities between the contact binary and MS functions (note in particular the dip at  $M_V = 7$  for BW<sub>3</sub>). However, there exist also some obvious differences between the shapes of  $LF_{BW}$  and  $LF_{MS}$ ; in particular, we see relatively fewer high-luminosity systems than low-luminosity ones, an effect which is stronger for the BW<sub>5</sub> sample. These differences can be ascribed to the fact that  $LF_{MS}$  is based on the local volume defined by the distance of less than 20 pc from the Sun, while the BW functions were obtained from a pencil-beam search reaching deep into the galactic space. If the contact binaries follow the distribution of disk stars, then we can expect changes in their numbers due to the structure of the galactic disk. This links the luminosity function and frequency of occurrence of contact binaries with the description of the galactic disk structure.

## 9. FREQUENCY OF OCCURRENCE OF CONTACT SYSTEMS

### 9.1. Influence of the galactic disk structure

The models of Bahcall & Soneira (1981) were used by Paczynski et al. (1994) to find out the numbers of disk stars along the OGLE line of sight. The same approach has been followed here with some minor modifications. The ratio of the star number density  $n(d)$  at a distance  $d$  to the local density  $n_0$  can be expressed as a product of two exponentials:  $c(d) = n(d)/n_0 = \exp(d/h_R) \exp(-|z|/h_z)$ , where  $h_R$  and  $h_z$  are the galactic disk length and height scales, respectively.  $h_z$  depends on the absolute magnitude of the MS stars as the galactic-plane concentration is spectral-type dependent. Bahcall (1986) suggested the following relations:  $h_z = 90$  pc for  $M_V < 2.3$  and  $h_z = 325$  pc for  $M_V > 5.1$ , with a linear interpolation between these values:  $h_z = 90 + 83.9(M_V - 2.3)$  pc. Paczynski et al. (1994) noted that for the galactic coordinates of the OGLE search ( $b \simeq -4^\circ$ , implying  $z \simeq 0.068 d$ ) and for  $h_R = 3.5$  kpc, the two exponential terms practically cancel out and the density stays approximately constant. However, the newest discussion of the galactic disk by Sackett (1997) suggests a shorter disk length scale,  $2.5 < h_R < 3.0$  kpc, so that the planar term may win leading to an increase in the numbers of stars at large distances. Since, as we argued in R97a, the contact binaries are apparently genuine members of the old disk population, the increase in star numbers along the OGLE line of sight for the shorter  $h_R$  could possibly explain the high numbers of contact binaries in the BW sample. The density change factors  $c(d) = n(d)/n_0$  are shown in Figure 13 for two values of  $h_R$ , 2.5 and 3.5 kpc. The shorter value of  $h_R$  results in a larger differentiation between the star number densities for various values of  $M_V$ . The decrease in numbers of early-type systems with distance is clearly visible for both values of  $h_R$ .

Comparison of the luminosity function for contact binaries with the local MS function requires knowledge of the mean weighted values of  $c(d)$  to the limits of 3 and 5 kpc, obtained by taking

into account the increasing volume with the distance. Because of this weighting, the systems at large distances contribute more to the mean densities obtained from the BW samples than the local systems. The weighted values of the factors  $c(d)$  for each bin of  $M_V$  can be calculated from:  $\bar{c}(d_l, h_R, h_z(M_V)) = \int_0^{d_l} c(\rho) \rho^2 d\rho / \int_0^{d_l} \rho^2 d\rho$ . The luminosity functions can now be related through  $\text{LF}_{BW}^{corr} = \text{LF}_{BW}^{obs} / \bar{c}(d_l, h_R, h_z)$ , and  $\text{LF}_{BW}^{corr} = \text{LF}_{MS} \times f$ , where  $f$  is the frequency of occurrence of contact binaries.  $d_l$  is the depth of the sample equal to respectively 3 or 5 kpc, while  $h_R$  have been assumed to be equal to 2.5 and 3.5 kpc;  $h_z(M_V)$  is given by the interpolation formula of Bahcall (1986) cited above. The corrected luminosity functions are given in Table 6.

The above formulation permits a comparison of the LF's for the contact binaries and the MS stars on the per  $M_V$ -bin basis. The frequencies  $f$  derived in such a way are shown in Figure 14 and are also listed in Table 7. The table gives the inverse apparent frequency of occurrence of contact binaries,  $1/f$ , expressed as the number of MS stars per one contact binary. The line WM gives the weighted mean values of the inverse frequencies over the available  $M_V$ . Because of the large errors in the first bin at  $M_V = 1$ , there are no changes in these frequencies if this bin is excluded from averaging. This bin is in fact affected by the bright limit of the OGLE survey. The bright limit of the sample at  $I \simeq 14.1$  (R97a) translates, for the average interstellar absorption in this direction, into the absolute magnitude limits for BW<sub>3</sub> and BW<sub>5</sub> of  $M_I \simeq 0.8$  and  $-0.3$ , respectively. Taking into account typical colors along the contact binary sequence, these upper limits correspond to  $M_V \simeq +1.0$  and  $-0.1$ . Thus, almost nothing can be said about the frequency of occurrence for  $M_V < 1.5$ . As we will see below in Section 9.4, the sky sample of bright systems gives us information that the frequency of contact binaries must fall down for such systems.

Except for the uncertainty at the bright end, Figure 14 shows that the corrections for the galactic structure produce the frequency distributions which are remarkably flat. The systematic differences in the luminosity function in Figure 12, which are best visible for intrinsically bright systems, are taken into account by the  $M_V$ -dependence of the disk height scale. It is possible that the corrections are too large for the bin at  $M_V = 2$ , but the data are consistent with the flat frequency distribution even for this bin. The resulting apparent frequency of the contact binaries in the BW direction is one system per about 130 MS stars for  $h_R = 2.5$  kpc and one system per about 100 MS stars for  $h_R = 3.5$  kpc. Unfortunately, at this stage, we cannot decide which number is the correct one. On one hand, uncertainties in the galactic disk structure are too large to make a preference with respect to  $h_R$ . On the other hand, we cannot use an argument that the contact binary frequency should have a flat distribution in  $M_V$  to determine  $h_R$ . Although our BW samples are perhaps among the first volume-limited ones in this particular galactic direction, we would not like to over-interpret the results as we feel that our crude interstellar-absorption model (R97a) may couple with the inferred spatial distribution of contact systems along the OGLE line of sight.

## 9.2. Frequency 1/130 or 1/100; why so high?

The frequency of occurrence of contact binaries in the BW samples of 1/130 or 1/100 that we have estimated above is some two times higher than the previous estimate of 1/250 – 1/300 that we obtained from the same BW material in R97a and for the old open clusters in CAL1. We will try to find explanations for these discrepancies in turn.

First of all, we should stress that the space density of contact binaries derived in R97a for BW<sub>3</sub>, to  $M_I = 4.5$  (or equivalently to  $M_V \simeq 5.5$ ) of  $7.6 \times 10^{-5}$  systems per pc<sup>3</sup> is a correct one. Paradoxically, the problem is with relating this number to the number of MS stars in the same volume. Since the numbers of stars that had been analyzed for variability by the OGLE project in successive apparent magnitude bins were not available, the numbers of stars with good photometry were used in R97a instead. For fainter magnitudes, the quality of photometry drops and the blending becomes more severe. We made therefore an assumption that the OGLE sample of stars with good photometry and the sample analyzed for variability had similar biases. The counting corrections for the good-photometry sample were quite large for fainter magnitudes, of the order of a factor of 2 or more, and this could be a source of a potentially large error. It is quite possible that the assumption of the identical character of biases in both samples was incorrect. The approach presented here is simpler: We find the BW luminosity function by simply counting the numbers of the contact systems, then correct it for the galactic disk structure and compare it with that for the MS stars from Wielen et al. (1983) by taking the ratio of the functions. If, for some reason, some contact systems are missed, we can only under-estimate their frequency of occurrence. As we discussed above, the main difficulty here is our insufficient knowledge of the disk length scale  $h_R$ , but the frequency comes out large for any of the two possible choices. Thus, we feel that the frequency for the BW sample is indeed high, about two times higher than estimated in R97a.

Concerning the frequencies observed in old open clusters: An earlier preliminary estimate of the apparent frequency in the clusters (CAL1) gave one contact system per  $275 \pm 75$  MS stars. This estimate was based on seven clusters of considerable spread in age from among the eleven that contribute to the present CL sample. As we know, we have good reasons to suspect that numbers of contact binaries increase with time. Therefore, the difference between the above estimate and the new determination for the BW sample may indicate an older – on the average – age of the latter sample. Estimates of the apparent frequency were published for two of the four clusters studied subsequently to CAL1, Cr 261 (Mazur et al. 1995) and NGC 7789 (Jahn et al. 1995). Depending how the cluster membership of the systems is established, the frequencies were found to be 1/140 – 1/88 for Cr 261 and 1/178 – 1/150 for NGC 7789. These determinations are in full agreement with our new value for the BW sample and with the frequency showing an increase with age because Cr 261 is an older cluster than NGC 7789.



### 9.3. Is there a low-luminosity end of the contact binary sequence?

The result on the high apparent frequency of incidence of contact systems in the BW sample is based primarily on the moderately bright among them, mostly within  $2.5 < M_V < 5.5$ . The volume corrections are large for systems fainter than  $M_V = 5.5$ , and there are no data for  $M_V > 7.5$ . However, we have no basis to assume that the contact binary sequence stops at  $M_V \simeq 7.5$  because we appear to see a few even fainter systems in the BW<sub>3</sub> sample (provided these are not artifacts of too red colors). Probably the only good argument for the existence of the sudden drop in the sequence is the constancy of the star number density when the limiting depth of the BW sample is evaluated for the depths of 3 and 2 kpc (R97a); apparently, no intrinsically faint systems (whose existence would produce a density increase for the smaller volume) have been detected in the solar neighborhood. However, the 2 kpc sample consist of only 27 objects, so that this argument is not very strong. Otherwise, the fact that we do not see faint contact systems may fall into the class of the *absence of evidence* versus *evidence of absence* reasoning. We do see a sharp end of the period distribution for both, BW<sub>3</sub> and CL, samples at about 0.225 day, but this is not an argument for a sharp cutoff in the absolute magnitude sequence as  $M_V$  changes very rapidly for short periods and red colors, where the period-color relation becomes almost vertical (see Figures 8 and 9). The period distribution is stretched for short periods when logarithmic units are used (see Figure 1) and there is more room for short-period systems. Arguably, the logarithmic units are the proper ones in view of the power-law dependencies governing the angular momentum loss.

The predictions based on the full convection limit (Rucinski 1992) place the expected low luminosity limit of the contact-binary sequence at  $B - V \simeq 1.5 - 1.6$ , that is at spectral types M2 – M4, leaving a large gap in the parameter space between the location of current “record holder”, CC Com<sup>4</sup> at  $(B - V)_0 = 1.24$  and  $P = 0.221$  day and the expected full-convection limit. We note that the close pair of M-type dwarfs, BW3.038 (Maceroni & Rucinski 1997) with the period of 0.1984 day, is on its way to becoming a contact system. Perhaps corresponding contact systems already exist and we simply have not found them? The fact that such faint systems have not been detected in the sky field is not an argument as the sky has been searched very poorly and unsystematically.

### 9.4. Comparison with the sky-field and cluster data

The variability amplitude distribution (Section 7), which is apparently biased to large values of the amplitudes, gives us a strong indication that many low inclination systems remain to be

---

<sup>4</sup>CC Coma, with its  $M_V = 6.7$  determined from the combined photometric and spectroscopic study of Rucinski et al. (1977) follows perfectly, to within 0.1 mag., the Hipparcos calibration CAL5. This is an argument that the calibration can be used for intrinsically faint systems.

discovered in the solar neighborhood. The pioneering study of Duerbeck (1984) attempted to correct for the orbital inclination discovery biases in the sky sample, leading to an estimate of the apparent frequency of occurrence of contact binaries of one system per about one thousand MS stars. In view of the subsequent work (CAL1, R97a), this estimate seemed too low by a factor of 3 – 4 times. Now, a new increase in the apparent frequency is postulated to the level of one contact system per about one hundred MS stars, a change which may be considered as quite drastic. Therefore, we must inquire whether the current results based on the BW sample are *consistent* with the sky field statistics.

With the luminosity functions in Table 6 or in Figure 12, one can easily calculate the number of stars in the “contact binary sky” by considering the space volume accessible for discoveries for a given limiting magnitude  $V_{lim}$ . We can use either the luminosity functions  $LF_3^{corr}$  or  $LF_5^{corr}$  or the scaled main-sequence function, recognizing that the latter has a smaller statistical uncertainties. Given a LF ( $M_V$ ), as in Table 5, one can calculate for each bin of  $M_V$  the total number of stars observable to a given apparent limiting magnitude  $V_{lim}$  from:  $n(M_V, V_{lim}) = LF(M_V) \times 4/3\pi d^3(M_V, V_{lim})$ , where  $d(M_V, V_{lim}) = 10^{1+0.2(V_{lim}-M_V)}$ . The examples for  $V_{lim} = 7.5$  (left vertical axis) and  $V_{lim} = 12.5$  (right vertical axis) are shown in Figure 15 for the MS luminosity function scaled by the factor of 130; for other  $V_{lim}$  the numbers can be obtained by the usual uniform spatial density scaling ( $10^3$  times per a five magnitude difference or 3.981 times per one magnitude). The last column of Table 5 gives  $n(M_V)$  for  $V_{lim} = 7.5$ .

How do the results compare with the data for the sky field? The predicted numbers of the faint end of contact systems are low, but – still – of the order of one hundred faint systems similar to CC Com are expected over the whole sky to  $V_{lim} = 12.5$ , in contrast to a dozen or so currently known. While there is no question that substantial contributions for a resolution of this discrepancy should come from large scale, yet simple surveys of the sky, similar to that currently conducted by Pojmanski (1997, 1998), a survey similar to OGLE, but deeper would probably offer a more efficient approach to learn about the faint end of the sequence. If the limit of OGLE were not  $I_{lim} = 17.9$ , but 19.9, we would already know the luminosity function beyond the position of CC Com.

The situation is very different at the bright end. The BW samples give us practically no information as only one, the same, contact system appears in both BW samples in the  $0.5 < M_V < 1.5$  bin, so that the sequence really starts with the bin  $1.5 < M_V < 2.5$ . This dearth of the systems is due to the bright limit of the OGLE survey at  $M_I \simeq 0.8$  and  $-0.3$ , for the  $BW_3$  and  $BW_5$  samples, respectively. Thus, we are forced to use the scaled MS data at the bright end and then check if the frequency scaling does apply here. We should note at this point that the CL sample has a bright end which is defined by the two brightest systems, HQ Mus and V732 Cas, at  $M_V = 2.0$ .

Figure 15 shows the well known fact that the visibility of stars in the sky is heavily biased toward intrinsically bright objects. The predictions based on the scaled MS data give  $40 \pm 7$

contact systems in the whole sky to  $V_{lim} = 7.5$ , but in that number as many as  $23 \pm 5$  would be contributed by the bin  $1.5 < M_V < 2.5$ . The additional  $10 \pm 2$  systems would come from the next bin  $2.5 < M_V < 3.5$  (see the last column of Table 5). If we eliminate the first bin at  $M_V = 2$ , the total number of systems with  $M_V > 2.5$  should be  $17 \pm 2$ . These predictions, when confronted with the observed numbers of contact binaries in the sky directly tell us that their frequency must decrease at high luminosities as we simply do not see that many bright contact binaries. At present, we know of one system at  $V = 4.7$  ( $\epsilon$  CrA), one system at  $V = 5.9$  (44i Boo B) and six further systems (S Ant, V535 Ara, RR Cen, VW Cep, AW UMa and HT Vir) are brighter than  $V_{lim} = 7.5$ . We know from the Hipparcos survey (CAL5, Duerbeck 1997) that most of them are indeed intrinsically luminous: Among those 8 systems, 6 fall in the interval  $1.5 < M_V < 3$ , while two (44i Boo B and VW Cep) have  $M_V > 5$ . Thus, we see about one half of the number of systems predicted by the high frequency of occurrence of  $1/130$ , but most of this discrepancy comes from the high luminosity end where the frequency must be definitely lower.

Let us assume that the number of contact binaries to  $V_{lim} = 7.5$  is indeed 8. We can learn about the discovery selection effects at fainter magnitudes by considering the numbers of systems predicted to various  $V_{lim}$ . For each magnitude increase, we expect an increase in the numbers of contact binaries by 3.981. Then, the sequence for the progression in the magnitude limits,  $V_{lim} = 7.5, 8.5, 9.5, 10.5, 11.5, 12.5$ , should lead to the predicted numbers of the systems to be 8, 32, 127, 505, 2009, 8000. Since we know some 600 contact binaries in the sky (some fraction of that in localized deep-search areas), we have a direct indication of discovery selection effects appearing at the level of about  $V_{lim} \simeq 10 - 11$ . Only wide field surveys can confirm or disprove this conjecture.

### 9.5. Comparison of the frequency of contact binaries to that of other MS binaries

When comparing the contact systems with other binaries we must remember that the former are located at the very end of the angular momentum and period sequences and we do not necessarily expect a perfect continuity over the whole range of orbital periods spanning several orders of magnitude. The currently best data on the period distribution for MS binaries are those by Duquennoy & Mayor (1991) who found that the distribution can be approximated, in the logarithm of the period, by a wide Gaussian with a maximum at  $\log P = 4.8$  and  $\sigma \log P = 2.3$ , with the period  $P$  expressed in days. Various techniques contributed to this result and the normalization of the distribution is somewhat uncertain. The recent results on the binarity of solar-type stars in the range where this distribution has a maximum (5 – 50 AU) offer a way of relatively reliable normalization of the distribution in the sense of spatial frequency (i.e. the frequency free of geometrical effects of unknown inclination). Patience et al. (1998) found that in the range of orbital periods,  $3.7 < \log P < 5.2$ , the frequency of incidence is  $0.14 \pm 0.03$  (this means that one among about 7 solar-type stars is a binary with a period in the range 14 – 430 years). This normalization has been used in Figure 16. In plotting the contact systems, it has been assumed that their total spatial frequency of occurrence is  $1/80$  which was (somewhat

conservatively) estimated to correspond to the apparent frequency of 1/130.

We clearly see in Figure 16 that the contact binaries with periods *shorter* than 0.6 – 0.7 day are very common forming a sharp peak extending well above the main-sequence relation. However, we should note the significant under-representation of contact systems with periods *longer* than 0.6 – 0.7 day. The latter can be detected to very large distances and are present in the OGLE sample, but they are very rare in terms of the spatial density. One would expect that, in a diagram like Figure 16, their place is occupied by close, short-period, detached binaries which have not yet lost enough angular momentum to enter into direct contact; however, no statistics similar to that available for contact binaries in Baade’s Window exists for such systems. Any attempts to find a trough in the period distribution on the long-period side of the contact-binary peak will obviously confront very different discovery selection effects for detached and contact eclipsing systems.

## 10. CONCLUSIONS

The main conclusion of this paper is that the two samples of disk population contact binaries give very similar results in almost every respect, in spite of very different origins of the samples. The similarities are observed in practically all distributions: those of the orbital periods and colors, of the luminosity functions and of the variability amplitudes. This is surprising and unexpected, as many observational effects would tend to make the distributions different. The CL sample would be expected to be particularly inhomogeneous as it was obtained by combining data for 11 different clusters ranging in age roughly by an order of magnitude, within 0.7 to 7 Gyr. Selection of these clusters was not systematic. In addition, they were observed to different limiting magnitudes, with various equipment and differing search areas. If any mass segregation would take place in a cluster, the CL sample should contain preferentially more massive systems, as typically only central parts of the clusters are only observed. Thus, we conclude that in spite of the small statistics – and possibly partly by coincidence – the available mixture of 11 clusters in the CL sample has been representative in the sense that it has not introduced its own observational biases. Thus, it would be hard to avoid a conclusion that it is the formation process of the contact systems which creates those same distributions irrespectively of the age of the population.

It has been found that contact systems typically appear in the period interval  $0.23 < P < 0.7$  day and the color interval  $0.3 < (B - V)_0 < 1.2$ . The turn-off points (TOP) of the clusters forming the CL sample all fall into the same color interval. However, the systems do not appear close to the respective TOP’s, but can appear anywhere in the above color range.

By comparing the galactic-disk corrected luminosity function derived from the BW sample with that for the MS stars in the solar neighborhood by Wielen et al. (1983), the apparent frequency of occurrence of contact systems in the interval  $2.5 < M_V < 7.5$  was found to be surprisingly high, at one contact system per about 130 main sequence stars of a given absolute magnitude for the galactic disk exponential length-scale  $h_R = 2.5$  kpc; the contact binaries would

be even more common, with the apparent frequency of one per about 100 MS stars for a longer scale of  $h_R = 3.5$  kpc. This high frequency is observed in the oldest among the open clusters such as Cr 261 or NGC 188, which suggests an advanced age of the BW sample systems. Total absence of contact systems in clusters younger than 0.7 Gyr and their low numbers in clusters younger than about 2 Gyr suggest a frequency of occurrence strongly dependent on the age of the stellar system. The reduction in the frequency for younger ages is difficult to quantify due to the low numbers of systems involved. The frequency of occurrence is at present the only property which appears to be different for the contact systems in old open clusters and in Baade’s Window.

The BW luminosity function determinations suffer from large search-volume corrections for  $M_V > 5.5$ , but they do cast doubt on the location of the faint end to the contact binary sequence, currently defined by the K5-type system CC Com at  $M_V = 6.7$ . The BW data do not extend above  $M_V \simeq +1.5$  so that the luminosity functions and frequencies of occurrence cannot be determined for intrinsically bright systems. However, the sky-field sample of bright stars to  $V_{lim} = 7.5$ , which presumably has been fully screened for the presence of contact systems, indicates a clear decrease in the apparent frequency for the high luminosity systems. This decrease cannot be quantified due to the small number statistics for the bright systems in the sky-field sample; a factor of two or three drop at  $M_V = 2$  is quite likely with much larger reductions for still brighter systems.

The limitations of this work are twofold: Because we are uncertain about the completeness for faint systems, we have not directly addressed the matter of the mass distribution of the contact systems, but this can be roughly estimated from the available  $M_V$  distributions and the diagram in the last panel in Figure 7. Also, since we have no idea about the mass-ratios of individual systems, we cannot say anything about the orbital angular momenta, which are dominated by the mass-ratio dependent term in:  $H \propto M^{5/3} P^{1/3} \frac{q}{(1+q)^2}$ .

This work does not include Population II contact systems of the type recently found in large numbers among blue stragglers of globular clusters (for most recent references, see Mateo (1996) and the new discoveries in  $\omega$  Cen and M4 by Kałuzny et al. (1997a, 1997b, 1997c)). However, halo-population stars are exceedingly rare in the solar vicinity, at the level of 0.125 - 0.15 percent of all stars (Bahcall 1986, Reid & Majewski 1993), so that no contact systems, even at high frequency of occurrence, would be expected among 98 members of our basic sample BW<sub>3</sub>. Thus, the results presented here are relevant solely to the most common contact binaries of the galactic disk field and of the old open clusters.

This work is dedicated to Janusz Kałuzny, my friend and colleague for over 20 years. Without his hard work, this study would have been entirely impossible.

Special thanks are due to Carla Maceroni and Hilmar Duerbeck for extensive and useful suggestions and comments on the first version of the paper.

## REFERENCES

- Bahcall, J.N. 1986, *ARA&A*, 24, 577
- Bahcall, J.N. & Soneira, R.M. 1980, *ApJS*, 44, 73
- Bessell, M.S. 1979, *PASP*, 91, 589
- Bessell, M.S. 1990, *A&AS*, 83, 357
- Duerbeck, H.W. 1984, *Ap&SS*, 99, 363
- Duerbeck, H.W. 1997, *Inf.Bull.Var Stars*, 4513
- Duquenois, A. & Mayor, M. 1991, *A&A*, 248, 485
- Eggleton, P.P. 1996, in *The Origins, Evolution, & Destinies of Binary Stars in Clusters*, eds. E.F. Milone & J.-C. Mermilliod, *ASP Conf.*, 90, 257
- Gilliland, R.L., Brown, T.M., Duncan, D.K., Suntzeff, N.B., Lockwood, G.W., Thompson, D.T., Schild, R.E., Jeffrey, W.A. & Penprase, B.E. 1991, *AJ*, 101, 541
- Guinan, E.F. & Bradstreet, D.H. 1988, in *Formation and Evolution of Low Mass Stars*, eds. A. K. Dupree & M. T. Lago (Kluwer, Dordrecht), p. 345
- Jahn, K., Kałużny, J. & Rucinski, S.M. 1995, *A&A*, 295, 101
- Kałużny, J. 1990, *AcA*, 40, 61
- Kałużny, J. & Shara, M.M. 1987, *ApJ*, 314, 585
- Kałużny, J. & Shara, M.M. 1988, *AJ*, 95, 785
- Kałużny, J. & Rucinski, S.M. 1993a, in *Blue Stragglers*, ed. R. A. Saffer (San Francisco, ASP), *ASP Conf.Ser.* 53, 164 (KR93)
- Kałużny, J. & Rucinski, S.M. 1993b, *MNRAS*, 265, 34
- Kałużny, J., Mazur, B. & Krzemiński, W. 1993, *MNRAS*, 262, 49
- Kałużny, J., Krzemiński, W. & Mazur, B. 1996, *A&AS*, 118, 303
- Kałużny, J., Thompson, I. & Krzemiński, W. 1997a, *AJ*, 113, 2219
- Kałużny, J., Kubiak, M., Szymański, M., Udalski, A. & Krzemiński, W. 1997b, *A&AS*, 120, 139
- Kałużny, J., Kubiak, M., Szymański, M., Udalski, A., Krzemiński, W. & Stanek, K. 1997c, *A&AS*, 122, 471
- Kazarovets, E.V., Samus, N.N. & Goranskij, V.P. 1993, *Inf.Bull.Var.Stars*, 3840
- Kazarovets, E.V. & Samus, N.N. 1995, *Inf.Bull.Var.Stars*, 4140
- Kazarovets, E.V. & Samus, N.N. 1997, *Inf.Bull.Var.Stars*, 4471
- Kroupa, P., Tout, C.A. & Gilmore, G. 1993, *MNRAS*, 262, 545
- Kubiak, M., Kałużny, J., Krzemiński, W. & Mateo, M. 1992, *AcA*, 42, 155

- Maceroni, C. & Rucinski, S.M. 1997, PASP, 109, 782
- Mateo, M. 1996, in *The Origins, Evolution, & Destinies of Binary Stars in Clusters*, eds. E.F. Milone & J.-C. Mermilliod, ASP Conf., 90, 21
- Mazur, B., Kałużny, J. & Krzemiński, W. 1993, MNRAS, 265, 405
- Mazur, B., Krzemiński, W. & Kałużny, J. 1995, MNRAS, 273, 59
- Milone, E.F., Stagg, C.R., Sugars, B.A., McVean, J.R., Schiller, S.J., Kallrath, J. & Bradstreet, D.H. 1995, AJ, 109, 359
- Paczynski, B., Stanek, K.Z., Udalski, A., Szymański, M., Kałużny, J., Kubiak, M., Mateo, M. & Krzemiński, W. 1994, AJ, 107, 2060
- Patience, J., Ghez, A.M., Reid, I.N., Weinberger, A.J. & Matthews, K. 1998, astro-ph/9801216 (Jan.98)
- Pojmański, G. 1997, AcA, 47, 467
- Pojmański, G. 1997, astro-ph/9802330 (Feb.98)
- Reid, N. & Majewski, S.R. 1993, ApJ, 409, 635
- Rucinski, S.M. 1977, PASP, 77, 888
- Rucinski, S.M. 1992, AJ, 103, 960
- Rucinski, S.M. 1993, in *The Realm of Interacting Binary Stars*, editors: J. Sahade, Y. Kondo & G. McClusky, (Netherlands: Kluwer Academic Publ.), p. 111
- Rucinski, S.M. 1994, PASP, 106, 462 (CAL1)
- Rucinski, S.M. 1995, PASP, 107, 648 (CAL2)
- Rucinski, S.M. 1997a, AJ, 113, 407 (R97a)
- Rucinski, S.M. 1997b, AJ, 113, 1112 (R97b)
- Rucinski, S.M. 1998, AJ, 115, 1135 (R98)
- Rucinski, S.M. & Duerbeck, H.W. 1997, PASP, 109, 1340 (CAL5)
- Rucinski, S.M. & Kałużny, J. 1994, Mem. Soc. Astr. Ital., 65, 113 (RK94)
- Rucinski, S.M., Kałużny, J. & Hilditch, R.W. 1996, MNRAS, 282, 705
- Rucinski, S.M., Whelan, J.A.J. & Worden, S.P. 1977, PASP, 89, 684
- Sackett, P.D. 1997, ApJ, 483, 103
- Twarog, B.A., Ashman, K.M. & Anthony-Twarog, B.J. 1997, AJ, 114, 2556
- Whelan, J.A.J., Worden, S.P. & Mochnacki, S.W. 1973, ApJ, 183, 133

Wielen, R., Jahreiss, H. & Krüger, R. 1983, in *The Nearby Stars and the Stellar Luminosity Function*, IAU Coll. 76, ed. A.G. Davis Philip and A.R. Upgren, (L. Davis Press, Inc., Schenectady, New York), p. 163



Figure captions:

Fig. 1.— The period distributions for the Baade’s Window 3 kpc ( $BW_3$ , continuous line), 5 kpc ( $BW_5$ , broken line), and open cluster (CL, hatched) samples, binned in linear (left panel) and logarithmic (right panel) units of the orbital period expressed in days. The histograms in this and the following figures are not normalized in order to visualize directly the numbers of systems in each bin and thus permit to judge the Poissonian errors in the distributions. Note that the left (CL) and right (BW) side vertical axes in this and the following figures are in proportion 3:2, to account approximately for the different sizes of the  $BW_3$  and CL samples of 98 and 63 systems. The data for 238 members of  $BW_5$  are shown scaled by 5 times, but the volume of  $BW_5$  is actually 4.6 times larger than that of  $BW_3$ .

Fig. 2.— The “period function”, PF, giving the number of detected systems in the  $BW_3$  (continuous line) and  $BW_5$  (broken line) samples in intervals of  $\Delta \log P = 0.1$  (in days) per unit of search volume. The vertical bars give the Poisson errors.

Fig. 3.— Same as in Figure 1 for the  $(B - V)_0$  color distributions. The vertical broken and dotted lines define the color ranges which contain 90 and all 98 systems of the  $BW_3$  sample. The tick marks in the upper edge of the figure give the spectral types following Bessell (1979).

Fig. 4.— The color–magnitude diagram for the  $BW_3$  sample, with the observed isochrones for Praesepe and NGC 6791 clusters shown by thin lines. The short vectors pointing down from the symbols give the light variation amplitudes multiplied by 3 times for better visibility. The amplitudes are discussed in Section 7. The two systems with unequally deep eclipses (Poor Thermal Contact binaries) are marked by open squares. The vertical broken lines mark the color ranges containing 90 percent of the  $BW_3$  systems. The insert at left shows the expected shifts in both coordinates due to the mass-ratio as it changes from  $q = 0$  to  $q = 1$ ; the tick marks along the line are placed at intervals of  $\Delta q = 0.2$ .

Fig. 5.— The color–magnitude diagrams for the 4 oldest clusters which are known to contain contact binaries: NGC 6791, Cr 261, NGC 188 and Be 39. The vertical broken and dotted lines give the 90-percent and full ranges for the  $BW_3$  sample. The PTC systems are marked by open squares. Light variation amplitudes are shown by downward pointing vectors; they are multiplied by 3 times to improve visibility (see Section 7). The observed isochrones for Praesepe and NGC 6791 clusters are shown by thin lines while the isochrone of each particular cluster is shown by a thick line. For each cluster, an estimated limit of the search for variability is indicated by a thin horizontal line in the lower part of the panel. The first panel gives the expected changes in position due to the unknown mass ratio, as in Figure 4.

Fig. 6.— Same as in the previous figure, but for M 67, NGC 2243, NGC 7789 and NGC 752.

Fig. 7.— Same as the two previous figures, but for the three “youngest” clusters of the CL sample: Tom 2, Praesepe and Be 33. It is possible that the only system visible in Be 33 does not actually

belong to it. The last panel of the figure shows the observed isochrone for Praesepe with the tick marks corresponding to  $0.25 M_{\odot}$  intervals of the mass of the primary component, as given by the mass–luminosity calibration for the disk stars by Kroupa et al. (1993). Changes due to the mass-ratio are shown by short curves which duplicate the insert in the first panel.

Fig. 8.— The period – color relation for the BW<sub>3</sub> sample, with data for contact binaries shown as filled circles. The open squares mark the two PTC systems in the sample. The curve gives the location of the SPBE for the  $B - V$  color,  $(B - V)_{SPBE} = 0.04 \times P^{-2.25}$ , which was determined to be consistent with the previously introduced in R97a for the  $V - I$  color (see the text). The previous relation, directly transformed from  $V - I$  to  $B - V$  is shown by a broken line. It is suspected that some of the systems appearing in the lower right area, below the slanted line, may have aliased periods and/or incorrect reddening values.

Fig. 9.— The period – color relation for the CL sample. Different symbols are used for each cluster, as explained in the legends to both panels, which give data separately for the oldest (upper panel) and the “youngest” (lower panel) clusters. The open symbols mark the PTC systems. The curve gives the approximation of the SPBE, as in the previous figure.

Fig. 10.— Comparison of the amplitude distributions for the BW<sub>3</sub> (line), CL (hatched) and sky-field (dotted) samples. The numbers for the sky sample have been scaled down by 3 times. Note the different scales used on both sides of the figure.

Fig. 11.— The distributions of the absolute magnitudes in the BW and CL samples. The format is similar to that used in Figures 1 and 2. The broken line gives the shape of the distribution for the BW<sub>5</sub> sample after scaling down by 5 times. The luminosity functions derived from both BW distributions are shown in the next figure.

Fig. 12.— The directly observed luminosity functions derived from the basic 3 kpc BW<sub>3</sub> sample (left panel) and the deeper 5 kpc BW<sub>5</sub> sample (right panel) are shown by continuous lines. The luminosity function for the local main sequence stars  $LF_{MS}$ , scaled down by a factor of 130, is plotted for comparison (dotted line in both panels). The vertical bars give the Poisson errors for individual bins. Beyond  $M_V > 5.5$  for BW<sub>3</sub> and  $M_V > 4.5$  for BW<sub>5</sub>, the plotted data include corrections for the progressively decreasing volumes; the uncorrected data are shown by thin broken lines. The bin  $3.5 < M_V < 4.5$  of BW<sub>5</sub> is partly affected by the finite depth of the search which is complete to  $M_V \simeq 4.2$ ; this difference has been disregarded here. Note that the luminosity functions shown here are not been corrected for the structure of the galactic disk. Such corrections require an assumption on the population characteristics of the contact binaries.

Fig. 13.— Ratios of the MS star number density for the galactic disk models to the local MS star density, for two values of the length scale  $h_R = 2.5$  and  $3.5$  kpc (left and right panels) and for three representative values of the scale height  $h_z(M_V) = 90, 190$  and  $325$  pc.

Fig. 14.— Apparent frequency of contact binary systems,  $f$ , relative to the number of MS stars

determined from the galactic structure corrected luminosity functions  $LF_{BW}^{corr}$ , for the two BW samples (3 kpc, upper row of panels; 5 kpc, lower row of panels) and for two values of the galactic length scale  $h_R$  (2.5 kpc, left panels; 3.5 kpc, right panels). The weighted mean values of the frequencies are shown by broken lines. The vertical bars give the errors determined for the inverse frequencies, as listed in Table 7.

Fig. 15.— The expected numbers of contact systems in one magnitude wide bins of  $M_V$ , in the whole sky to the limiting magnitudes  $V_{lim} = 7.5$  (left vertical axis) and  $V_{lim} = 12.5$  (right vertical axis), predicted from the main-sequence luminosity function and scaled down by 130, are shown by the continuous line histogram. The currently known numbers of the systems to  $V_{lim} = 7.5$  are shown by a broken line. The non-detections are plotted at the level of  $1 \pm 1$  which is plausible from the point of view of the Poissonian-statistics in the adjacent bins. The figure suggests a decrease in the frequency of occurrence for  $M_V < 3.5$ , whereas the BW data (see Figure 14) are consistent with the frequency staying constant for  $M_V > 2.5$ .

Fig. 16.— The observed spatial (free of geometric and inclination effects) frequency of occurrence of disk binary systems following the study of Duquennoy & Mayor (1991) is shown as one branch of a Gaussian curve, with the logarithmic units of the period in days. It has been normalized to give the integrated observed frequency in the range  $3.7 < \log P(d) < 5.2$  of 0.14, following the study of Patience et al. (1998). The histograms for the contact systems in the BW<sub>3</sub> (continuous line) and BW<sub>5</sub> (broken line) samples have been copied from the period function in Figure 2 after normalization to give the integrated spatial frequency of occurrence of contact binaries equal to 1/80 (about 1.5 higher than the apparent frequency). This conversion is approximate with the combined uncertainty in the spatial frequency of contact binaries relative to main sequence stars of about 50 percent.



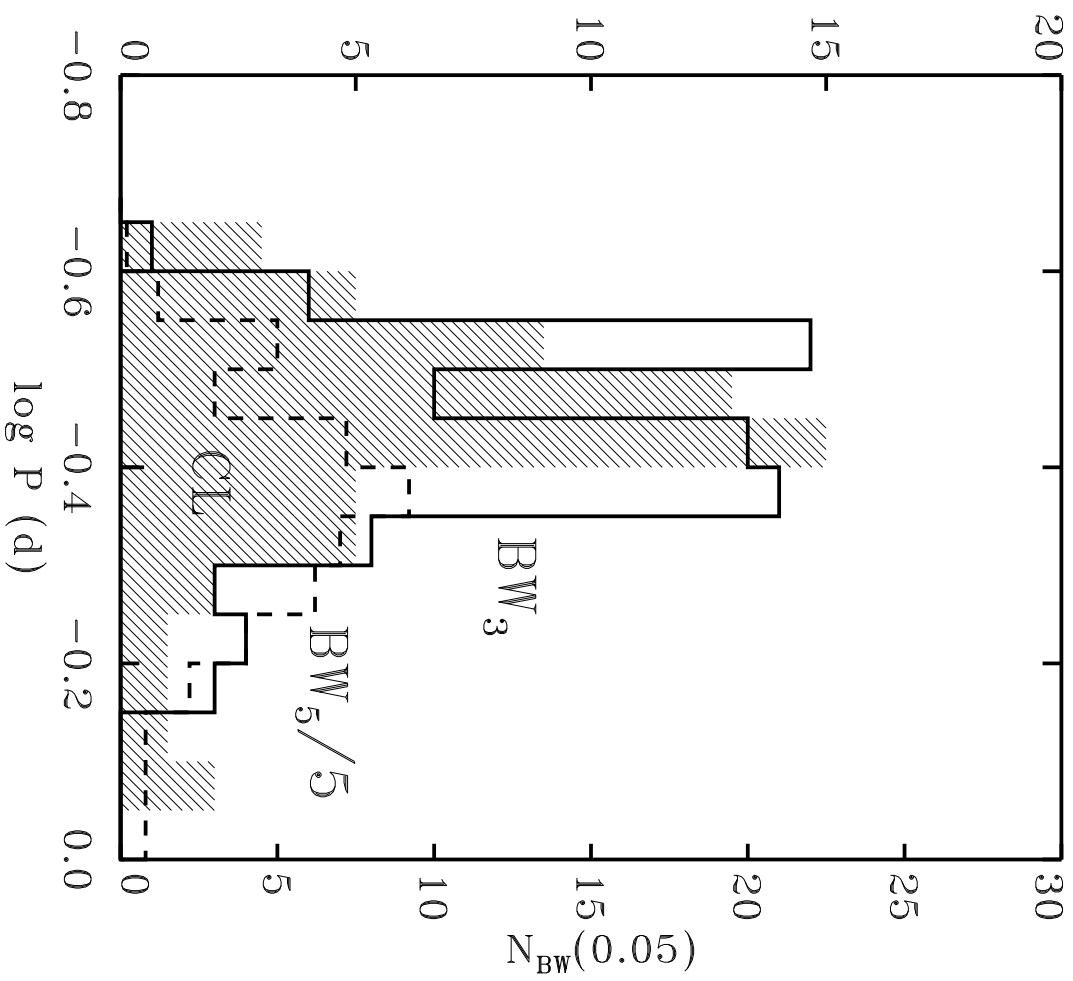
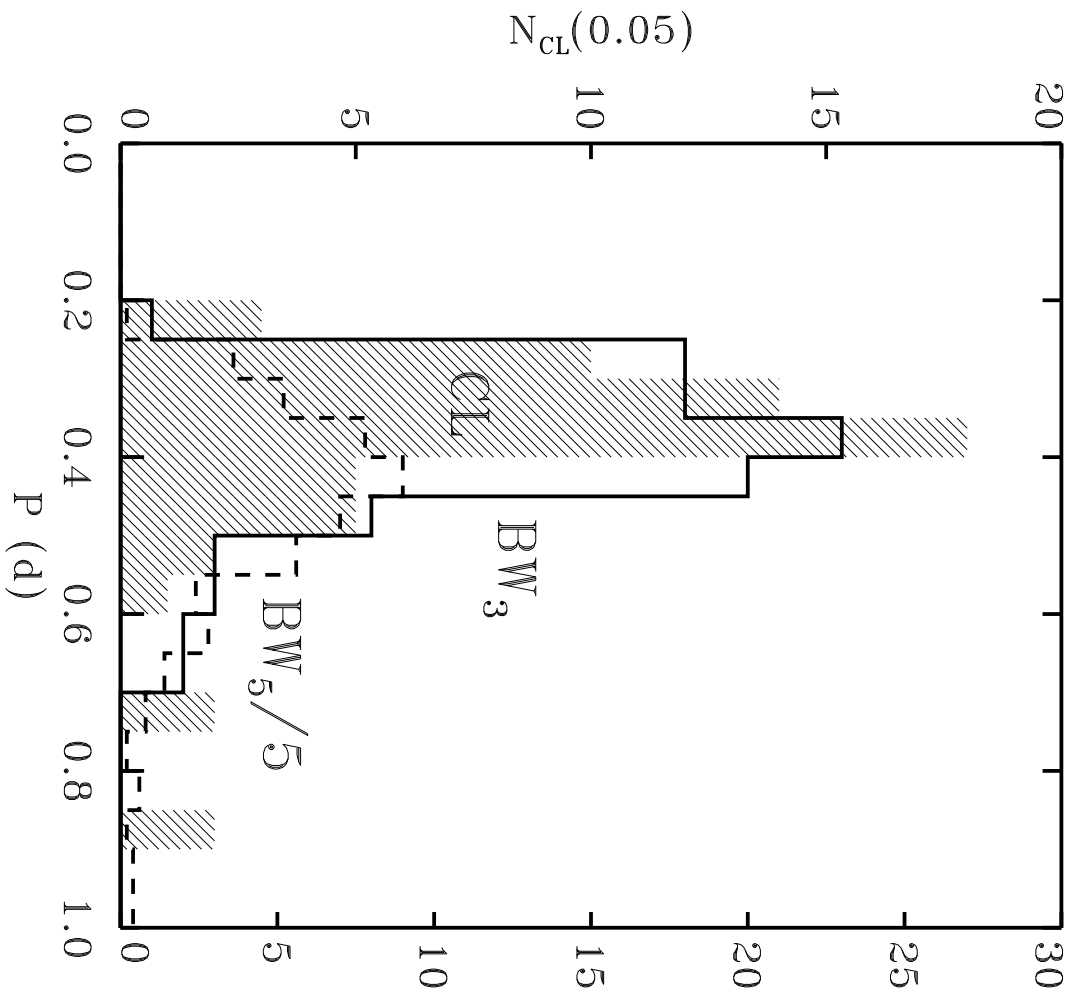


TABLE 1. Baade's Window Volume-Limited 3 kpc Sample (BW<sub>3</sub>)

BW	P(day)	$I_{max}$	$V - I$	Ampl <sub>I</sub>	$E_{V-I}$	$M_V$	$(B - V)_0$
0.004	0.4026	14.63	1.15	0.19	0.46	3.89	0.63
0.050	0.3973	15.68	1.09	0.16	0.59	3.29	0.43
0.057	0.3414	15.74	1.52	0.27	0.47	5.42	0.97
0.068	0.3486	16.02	1.55	0.16	0.54	5.23	0.94
0.088	0.4146	16.30	1.34	0.36	0.66	3.80	0.62
0.092	0.4674	16.42	1.42	0.35	0.64	3.88	0.72
0.093	0.4114	16.42	1.39	0.25	0.64	4.06	0.69
0.109	0.2890	16.71	1.73	0.24	0.47	6.43	1.13
0.110	0.4165	16.71	1.45	0.48	0.66	4.14	0.73
0.115	0.3025	16.79	1.51	0.29	0.70	4.86	0.75
0.118	0.2515	16.85	1.20	0.14	0.56	4.66	0.58
0.121	0.3244	16.87	1.57	0.21	0.60	5.25	0.91
0.128	0.3833	16.94	1.53	0.43	0.69	4.48	0.78
0.169	0.3526	17.35	1.89	0.20	0.60	6.13	1.15
1.003	0.5062	14.36	0.99	0.15	0.58	2.53	0.35
1.016	0.4063	15.16	1.23	0.24	0.55	3.84	0.62
1.038	0.4814	15.67	1.25	0.52	0.64	3.27	0.55
1.048	0.4419	15.91	1.17	0.44	0.63	3.21	0.48
1.052	0.2834	15.96	1.24	0.13	0.59	4.46	0.59
1.084	0.4021	16.41	1.27	0.47	0.59	3.87	0.63
1.096	0.3566	16.56	1.54	0.31	0.71	4.59	0.77
1.160	0.3144	17.18	1.52	0.26	0.65	4.99	0.82
1.165	0.2881	17.27	1.58	0.23	0.61	5.47	0.91
1.173	0.3139	17.36	1.59	0.23	0.65	5.22	0.89
1.181	0.3331	17.43	1.74	0.20	0.66	5.58	1.00
2.006	0.3604	14.79	1.11	0.36	0.48	3.93	0.58
2.082	0.3849	16.84	1.66	0.82	0.72	4.80	0.89
2.091	0.3984	16.93	1.71	0.39	0.74	4.83	0.91
2.095	0.3137	16.96	1.44	0.27	0.72	4.50	0.66
2.116	0.4065	17.20	1.68	0.31	0.68	4.89	0.93
2.161	0.2995	17.72	1.73	0.33	0.68	5.68	0.97
2.167	0.3033	17.80	1.68	0.25	0.67	5.52	0.94
3.003	0.6604	14.23	0.92	0.40	0.71	1.32	0.19
3.007	0.5728	14.73	1.03	0.37	0.73	1.90	0.25
3.008	0.3072	14.88	1.09	0.52	0.52	4.03	0.51
3.012	0.3698	15.13	1.27	0.41	0.74	3.54	0.47
3.018	0.3111	15.50	1.23	0.28	0.55	4.39	0.63
3.020	0.2967	15.56	1.14	0.35	0.61	3.96	0.46
3.022	0.6097	15.60	1.51	0.12	0.67	3.55	0.78
3.024	0.3977	15.66	1.39	0.18	1.01	2.90	0.32
3.039	0.3358	15.87	1.16	0.26	0.67	3.59	0.42
3.053	0.4659	15.99	2.59	0.45	0.28	8.93	1.54
3.056	0.3900	16.04	1.32	0.23	0.77	3.48	0.48
3.097	0.3608	16.68	1.45	0.42	0.65	4.47	0.74
3.139	0.3223	17.19	1.46	0.40	0.75	4.39	0.65
3.148	0.2889	17.36	1.90	0.43	0.87	5.68	0.96
3.193	0.2658	17.77	1.57	0.36	0.69	5.34	0.82
4.010	0.4236	15.16	1.02	0.50	0.76	2.38	0.23
4.015	0.4209	15.25	1.08	0.10	0.61	3.06	0.40
4.016	0.3760	15.25	1.14	0.32	0.66	3.34	0.42
4.017	0.4575	15.42	1.29	0.26	0.68	3.38	0.56
4.020	0.4199	15.46	1.22	0.27	0.71	3.22	0.45

TABLE 1. (continued)

BW	P(day)	$I_{max}$	$V - I$	Ampl $_I$	$E_{V-I}$	$M_V$	$(B - V)_0$
4.032	0.4062	15.69	1.30	0.37	0.65	3.73	0.59
4.040	0.2277	15.72	1.69	0.46	0.27	7.45	1.24
4.042	0.4384	15.77	1.35	0.10	0.69	3.61	0.60
4.067	0.4665	16.33	1.59	0.36	0.67	4.37	0.87
4.075	0.2783	16.39	1.32	0.43	0.66	4.53	0.60
4.076	0.3758	16.39	1.39	0.13	0.70	4.03	0.63
4.096	0.2963	16.60	1.46	0.45	0.67	4.84	0.73
4.141	0.4008	17.18	1.65	0.19	0.66	4.89	0.93
4.154	0.4011	17.31	1.87	0.27	0.67	5.58	1.08
4.161	0.2977	17.42	1.65	0.52	0.67	5.45	0.92
4.172	0.3890	17.50	1.80	0.23	0.69	5.35	1.02
5.007	0.5418	14.33	0.87	0.33	0.64	1.78	0.20
5.037	0.4413	15.70	1.52	0.23	0.78	3.86	0.68
5.075	0.6449	16.38	1.71	0.23	0.70	4.02	0.95
5.076	0.2834	16.41	1.39	0.13	0.69	4.64	0.65
5.077	0.3506	16.41	1.36	0.81	0.64	4.27	0.66
5.114	0.2600	17.09	1.80	0.34	0.50	6.79	1.16
5.143	0.4815	17.51	2.00	0.32	0.70	5.54	1.15
5.145	0.3159	17.55	1.77	0.32	0.67	5.75	1.02
5.157	0.4706	17.65	1.96	0.29	0.68	5.54	1.14
5.163	0.3622	17.75	1.87	0.30	0.80	5.37	0.99
6.005	0.6984	14.78	1.25	0.35	0.81	1.96	0.37
6.019	0.5647	15.41	1.16	0.22	0.68	2.53	0.42
6.041	0.2869	15.85	1.39	0.44	0.45	5.39	0.89
6.056	0.2670	16.14	1.40	0.11	0.55	5.25	0.80
6.060	0.3406	16.22	1.60	0.28	0.59	5.27	0.94
6.071	0.3909	16.48	1.59	0.61	0.68	4.66	0.85
6.086	0.3768	16.86	1.53	0.26	0.75	4.33	0.72
6.123	0.5399	17.38	2.07	0.29	0.73	5.46	1.19
7.040	0.3846	15.83	1.12	0.33	0.62	3.37	0.44
7.045	0.3040	16.02	1.44	0.16	0.55	5.10	0.83
7.086	0.3371	16.72	1.49	0.50	0.67	4.66	0.76
7.112	0.5900	17.09	2.58	0.17	0.49	7.76	1.51
7.124	0.4173	17.27	1.71	0.27	0.68	4.95	0.96
7.132	0.4306	17.34	1.80	0.23	0.69	5.16	1.02
7.147	0.4920	17.50	1.97	0.33	0.63	5.65	1.19
7.153	0.2734	17.64	1.72	0.20	0.62	6.02	1.01
8.005	0.4370	14.64	1.01	0.45	0.50	3.13	0.44
8.027	0.3600	15.44	1.11	0.42	0.70	3.21	0.35
8.031	0.4435	15.48	1.02	0.39	0.55	2.96	0.40
8.045	0.3012	15.92	1.25	0.33	0.53	4.56	0.66
8.050	0.3766	16.09	1.37	0.26	0.73	3.85	0.58
8.072	0.2838	16.54	2.04	0.54	0.27	8.15	1.40
8.095	0.3675	17.02	1.64	0.32	0.56	5.36	1.00
8.106	0.3818	17.15	1.68	0.29	0.79	4.67	0.84
8.138	0.2877	17.64	1.72	0.46	0.56	6.12	1.06

Notes to Table 1.

The first 5 columns are quoted from the OGLE catalog, while the last 3 columns give the derived data, as described in R97a.

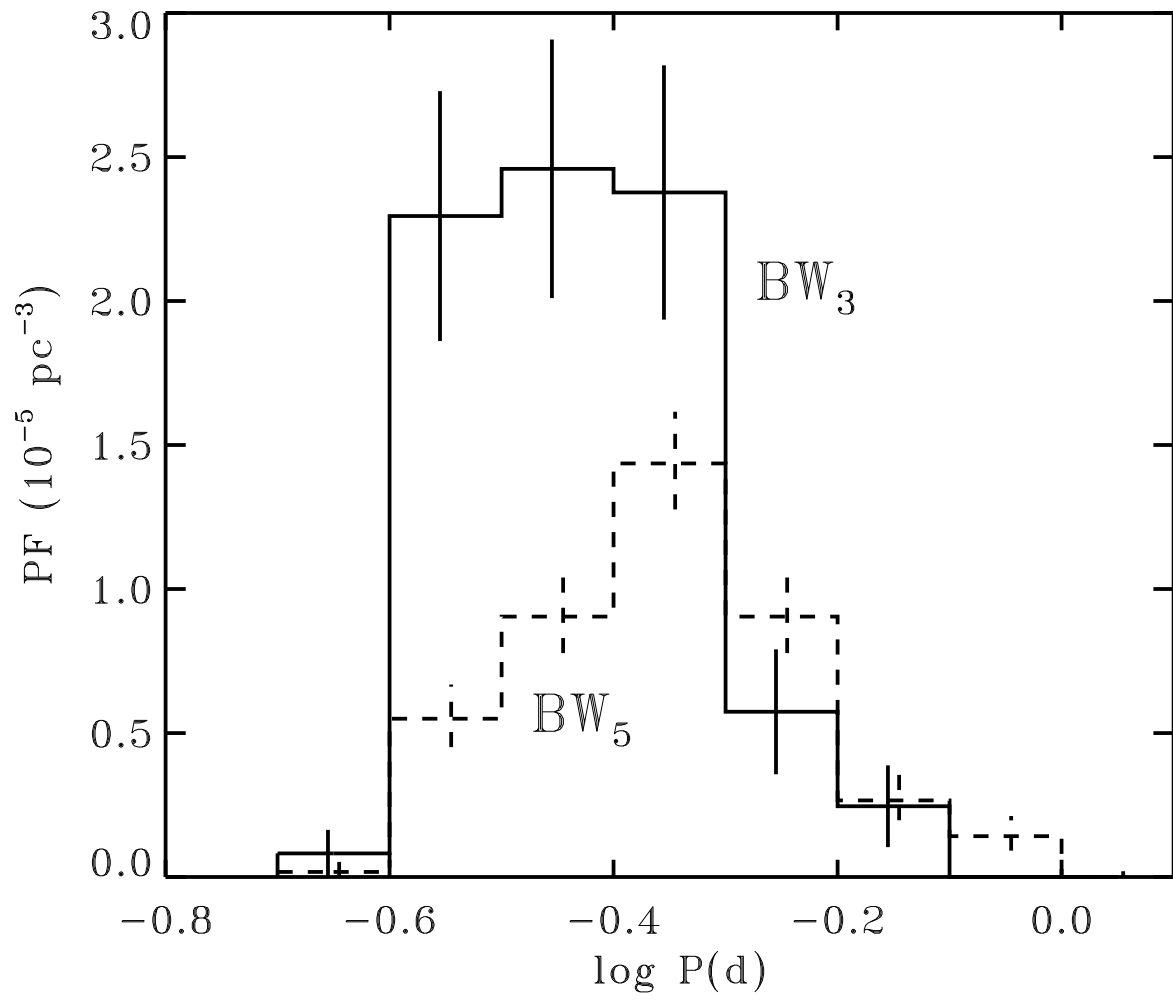




TABLE 2. Open clusters with contact systems (CL)

Name	Age (Gyr)	$(m - M)_V$	$E_{B-V}$	[Fe/H]	$b(\text{deg})$	$M_V^{lim}$	Memb	Non-m	Ref
NGC 6791	7	13.4	0.15	+0.15	+11	6.3	4	4	1, 2
Cr 261	7	13.0	0.22	...	-6	6.6	25	3	3
NGC 188	6	11.35	0.10	-0.03	+22	7.4	7		4, 5
Be 39	6	13.50	0.11	-0.18	+10	7.0	9	2	6
M 67	5	9.80	0.04	0	+32	>8	3		7
NGC 2243	3	13.45	0.06	-0.44	-18	6.6	2		8
NGC 7789	2	12.45	0.30	-0.08	-5	7.1	6	1	9
NGC 752	2	8.35	0.04	-0.09	+23	6.7	1		10
Tom 2	1	15.6	0.30	-0.36	-7	5.2	4		11
Praesepe	0.9	6.40	0.	+0.14	+32	6.6	1		12
Be 33	0.7	15.5:	0.7:	-0.6 :	-5	5.0	(1)		13

## References for Table 2.

References to papers with studies of W UMa systems: (1) Kałuzny & Rucinski 1993b; (2) Rucinski et al. 1996; (3) Mazur et al. 1995; (4) Kałuzny & Shara 1987; (5) Kałuzny 1990; (6) Kałuzny et al. 1993; (7) Gilliland et al. 1991; (8) Kałuzny et al. 1996; (9) Jahn et al. 1995; (10) Milone et al. 1995; (11) Kubiak et al. 1992; (12) Whelan et al. 1973; (13) Mazur et al. 1993.

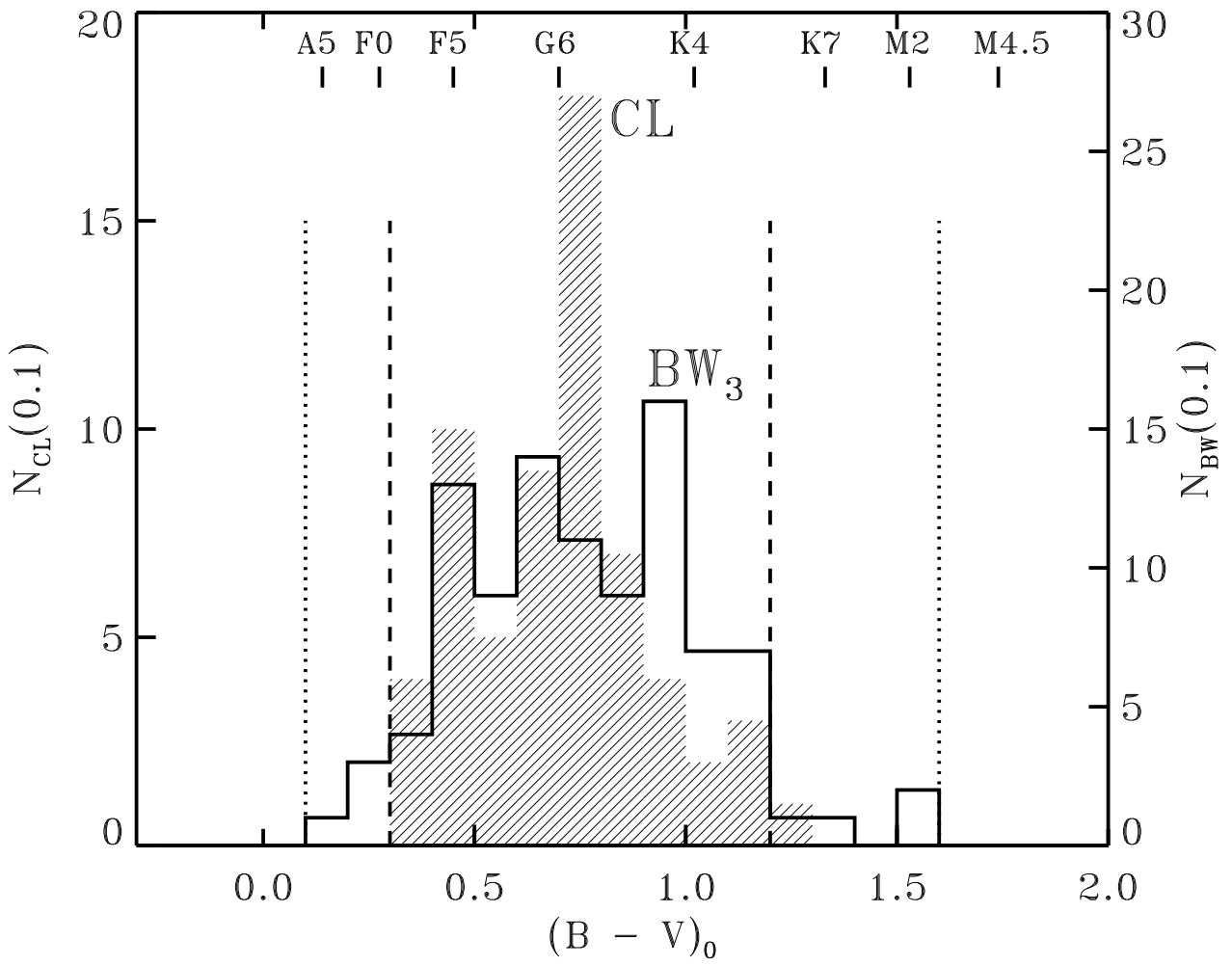


TABLE 3. W UMa-type Systems in Open Clusters (CL)

Name <sub>1</sub>	Name <sub>2</sub>	P(day)	$V_{max}$	$B - V$	$M_V$	$\Delta M_V$	Ampl <sub>V</sub>	Comm
<b>NGC 6791</b>								
V513 Lyr	V7	0.3935	17.69	0.87	4.19	0.16	0.17	
V514 Lyr	V8	0.4000	17.66	1.27	4.16	-1.05	0.11	nm
V518 Lyr	V5	0.3130	17.21	0.87	3.71	-0.76	0.05	
V519 Lyr	V1	0.2677	16.22	0.85	2.72	-1.99	0.40	nm
V521 Lyr	V4	0.3255	17.78	0.93	4.28	-0.30	0.11	
V522 Lyr	V6	0.2797	15.45	0.70	1.95	-2.23	0.12	nm
V525 Lyr	V3	0.3180	18.61	1.01	5.11	0.24	0.10	
V526 Lyr	V2	0.3170	19.70	0.98	6.20	1.42	0.10	nm
<b>Cr 261</b>								
GV Mus	V36	0.4320	17.80	0.98	4.80	0.77	0.15	
GW Mus	V41	0.2630	19.16	1.20	6.16	0.51	0.20	
GX Mus	V4	0.3817	16.81	0.96	3.81	-0.40	0.30	
GY Mus	V2	0.3550	16.74	1.04	3.74	-0.85	0.08	
GZ Mus	V30	0.3513	17.02	0.86	4.02	-0.05	0.40	
HK Mus	V10	0.3808	19.30	1.34	6.30	0.94	0.45	
HL Mus	V26	0.4613	15.55	0.72	2.55	-0.57	0.25	
HM Mus	V19	0.3431	17.42	1.12	4.42	-0.48	0.60	
HO Mus	V17	0.4571	15.85	0.78	2.85	-0.47	0.12	
HQ Mus	V16	0.8841	14.99	0.73	1.99	0.09	0.35	
HU Mus	V32	0.5190	15.52	0.64	2.52	-0.13	0.12	
HV Mus	V31	0.3820	16.70	0.99	3.70	-0.60	0.05	
HX Mus	V35	0.3697	19.42	1.12	6.42	1.66	0.60	nm
HY Mus	V9	0.4114	18.67	1.06	5.67	1.30	0.25	nm
HZ Mus	V37	0.4295	15.97	0.82	2.97	-0.59	0.13	
II Mus	V28	0.3845	17.30	1.02	4.30	-0.08	0.17	
IK Mus	V13	0.3749	17.29	1.00	4.29	-0.08	0.65	
IL Mus	V33	0.2900	18.24	1.09	5.24	0.11	0.80	
IO Mus	V25	0.4009	16.38	0.88	3.38	-0.50	0.30	
IR Mus	V15	0.3158	18.04	1.22	5.04	-0.32	0.55	
IS Mus	V18	0.3454	19.20	1.39	6.20	0.50	0.80	
IT Mus	V34	0.3727	18.90	0.99	5.90	1.55	0.20	nm
IU Mus	V14	0.2638	19.40	1.41	6.40	0.12	0.40	
IW Mus	V24	0.3544	16.84	1.02	3.84	-0.70	0.13	
IX Mus	V1	0.3780	17.84	0.94	4.84	0.67	0.25	
IZ Mus	V3	0.3916	18.15	1.15	5.15	0.41	0.60	
KL Mus	V43	0.3730	16.48	0.83	3.48	-0.38	0.05	
KM Mus	V39	0.4307	17.24	0.82	4.24	0.68	0.30	
<b>NGC 188</b>								
EP Cep		0.2897	16.50	0.95	5.00	-0.08	0.45	
EQ Cep		0.3069	16.42	0.92	4.92	0.05	0.79	
ER Cep		0.2857	15.60	0.83	4.10	-0.64	0.82	
ES Cep		0.3424	15.60	0.85	4.10	-0.35	0.50	
V369 Cep	V7	0.3282	16.00	0.82	4.50	0.06	0.65	
V370 Cep	V6	0.3304	16.08	0.83	4.58	0.12	0.15	
V371 Cep	V5	0.5860	15.87	0.92	4.37	0.74	0.33	

TABLE 3. (continued)

Name <sub>1</sub>	Name <sub>2</sub>	P(day)	$V_{max}$	$B - V$	$M_V$	$\Delta M_V$	Ampl <sub>V</sub>	Comm
<b>Be 39</b>								
V701 Mon	V10	0.5460	15.94	0.50	2.54	0.11	0.35	
V702 Mon	V11	0.2254	19.62	1.33	6.22	-0.43	0.44	
V703 Mon	V8	0.2288	19.16	1.19	5.76	-0.44	0.77	
V704 Mon	V7	0.2780	18.34	0.90	4.94	0.00	0.43	
V705 Mon	V3	0.3810	16.82	0.58	3.42	0.05	0.07	
V706 Mon	V2	0.4865	16.16	0.70	2.76	-0.50	0.22	
V707 Mon	V9	0.2598	20.12	0.95	6.72	1.49	1.00	nm
V709 Mon	V4	0.3813	17.10	0.69	3.70	0.00	0.51	
V710 Mon	V1	0.4052	15.36	0.58	1.96	-1.29	0.41	nm
V711 Mon	V5	0.2656	18.04	0.88	4.64	-0.33	0.13	
V712 Mon	V6	0.2844	18.11	0.85	4.71	-0.04	0.34	
<b>M 67</b>								
AH Cnc	III-33	0.3604	13.31	0.54	3.72	0.15	0.38	
ET Cnc	III-79	0.2704	15.81	1.10	6.22	0.41	0.14	
EV Cnc	III-2	0.4412	12.74	0.45	3.15	0.24	0.15	
<b>NGC 2243</b>								
	V2	0.2853	17.82	0.78	4.72	0.02	0.22	nd
	V3	0.3564	16.66	0.55	3.56	-0.01	0.30	nd
<b>NGC 7789</b>								
V730 Cas	V6	0.8840	14.54	0.62	2.24	0.73	0.05	
V732 Cas	V1	1.1900	14.26	0.68	1.96	0.85	0.16	
V733 Cas	V7	0.4550	15.93	0.93	3.63	-0.09	0.06	
V736 Cas	V2	0.7200	14.81	0.69	2.51	0.40	0.16	
V737 Cas	V4	0.3370	16.72	1.05	4.42	-0.24	0.14	
V738 Cas	V5	0.2387	19.32	1.20	7.02	1.24	0.40	nm
	V3	0.7000	15.30	0.69	3.00	0.83	0.07	nd
<b>NGC 752</b>								
QX And	H235	0.4118	11.28	0.44	2.93	-0.14	0.21	
<b>Tom 2</b>								
	V2	0.3278	20.19	1.02	4.69	0.55	0.35	nd
	V3	0.4712	18.79	0.84	3.29	0.39	0.29	nd
	V4	0.3105	19.80	0.71	4.30	0.99	0.18	nd
	V5	0.3533	19.32	0.79	3.82	0.52	0.36	nd
<b>Praesepe</b>								
TX Cnc		0.3829	10.02	0.62	3.78	-0.06	0.35	
<b>Be 33</b>								
II CMa	V1	0.2292	15.22	1.30	-0.28	-5.05	0.50	nm
IK CMa	V2	0.3262	18.00	1.12	2.50	-1.05	0.46	xx

Notes to Table 3.

Last column: nm – non member; nd – no designation as variable star available; xx – formally not fulfilling the membership criterion, of  $|\Delta M_V| < 1$  mag, but included in the CL sample.  $\Delta M_V = M_V - M_V^{cal}$ , where  $M_V = V_{max} - (m - M)_V$ , the distance moduli are given in Table 2 and  $M_V^{cal}$  come from the Hipparcos calibration.

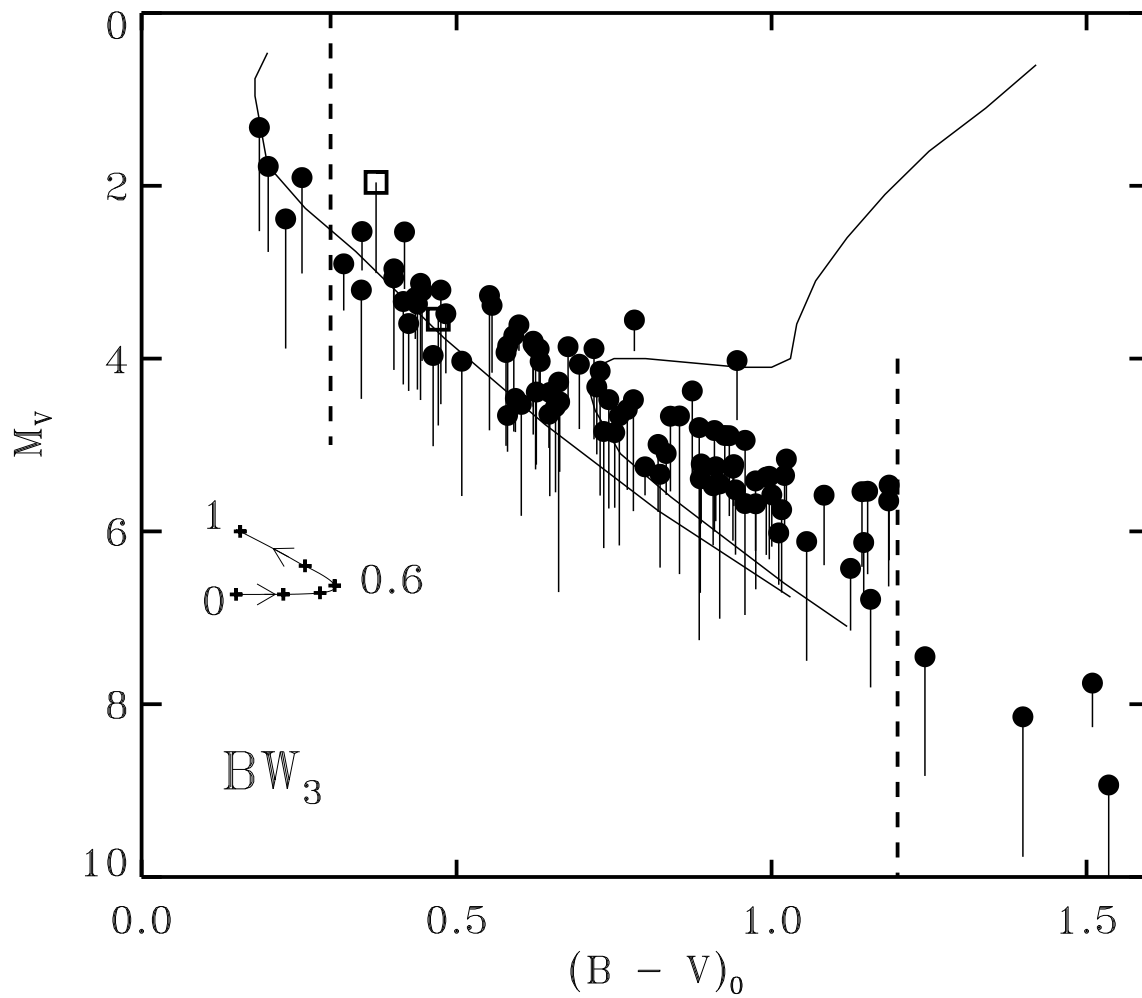


TABLE 4. Period function

$\log P$ (days)	$N_3$	$N_5$	$PF_3$ ( $10^{-5}\text{pc}^{-3}$ )	$PF_5$ ( $10^{-5}\text{pc}^{-3}$ )
-0.7 ... -0.6	1	1	0.082	[0.018]
-0.6 ... -0.5	28	31	2.30	[0.55]
-0.5 ... -0.4	30	51	2.46	[0.90]
-0.4 ... -0.3	29	81	2.38	[1.44]
-0.3 ... -0.2	7	51	0.57	[0.90]
-0.2 ... -0.1	3	15	0.25	0.26
-0.1 ... 0.0	0	8	0	0.14

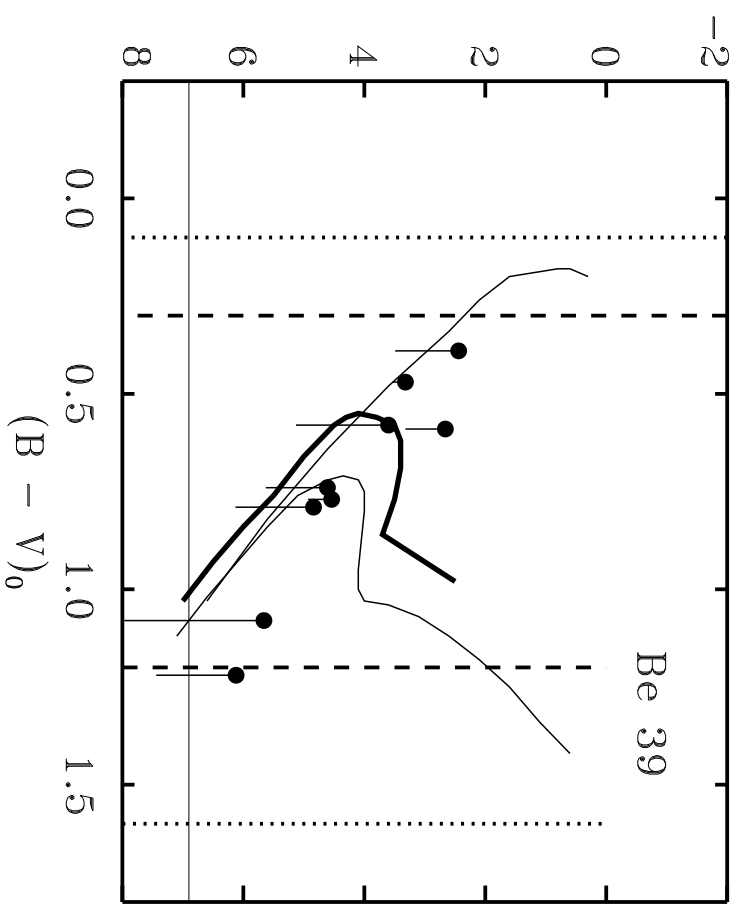
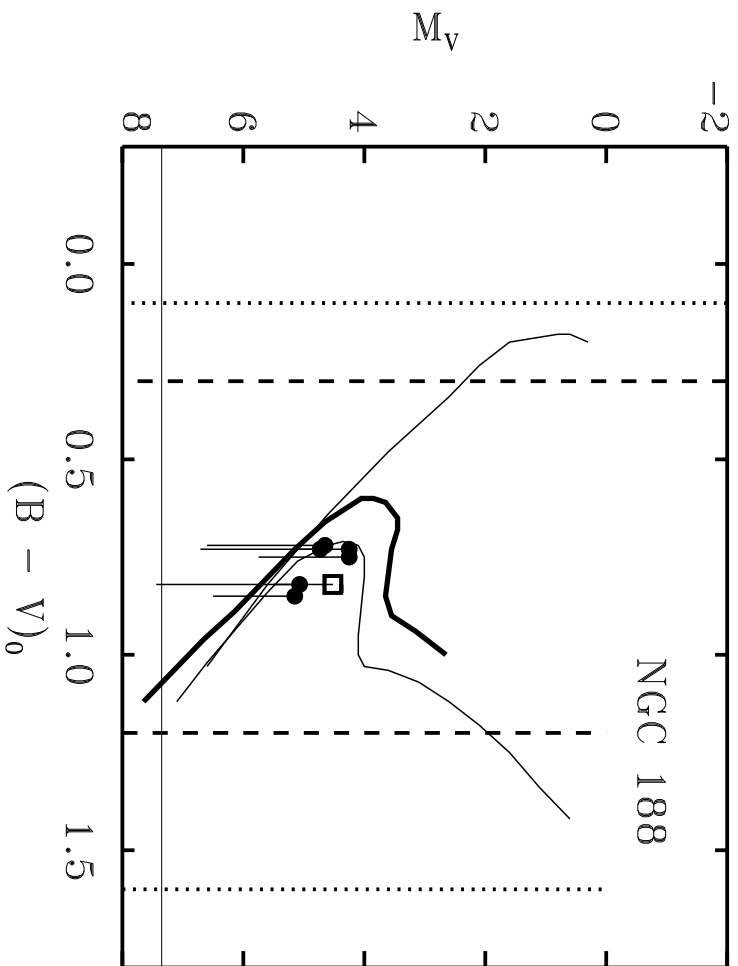
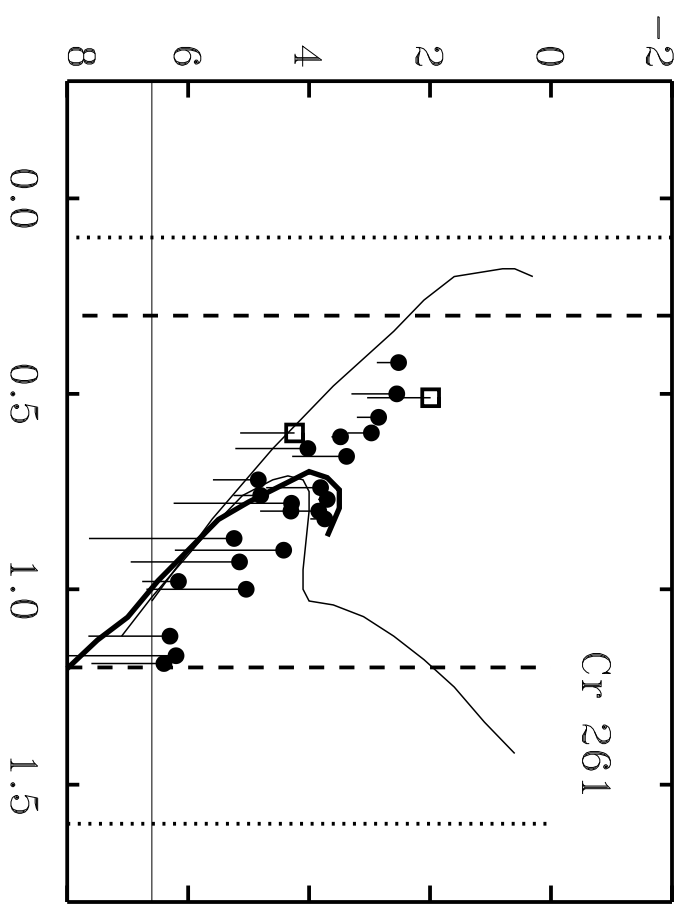
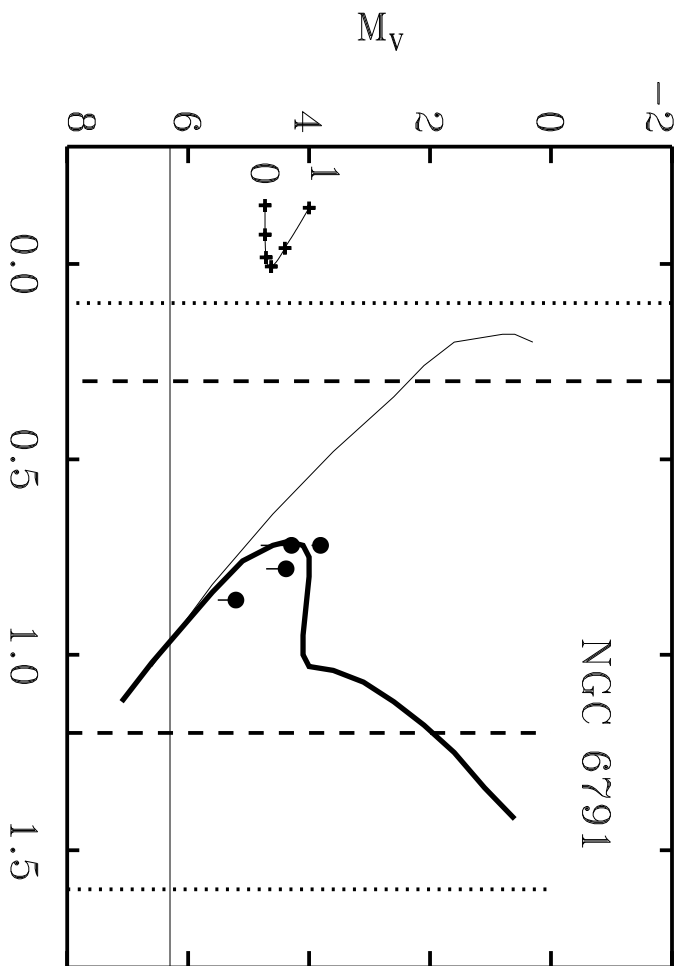


TABLE 5. Observed luminosity function

$M_V$	$N_3$	$N_5$	$LF_3^{obs}$ ( $10^{-5}\text{pc}^{-3}$ )	$LF_5^{obs}$ ( $10^{-5}\text{pc}^{-3}$ )	$LF_{MS}$ ( $10^{-5}\text{pc}^{-3}$ )	$n_{MS}(7.5)/130$
1	1	1	$0.08 \pm 0.08$	$0.018 \pm 0.018$	$0.32 \pm 0.08$	$54 \pm 14$
2	4	18	$0.33 \pm 0.16$	$0.32 \pm 0.08$	$0.55 \pm 0.11$	$23.1 \pm 5.0$
3	15	42	$1.23 \pm 0.32$	$0.74 \pm 0.12$	$0.99 \pm 0.15$	$10.4 \pm 1.6$
4	28	105	$2.30 \pm 0.43$	$1.86 \pm 0.18$ <sup>a</sup>	$1.79 \pm 0.20$	$4.7 \pm 0.5$
5	32	54	$2.63 \pm 0.46$	$[3.8 \pm 0.5]$	$2.48 \pm 0.24$	$1.65 \pm 0.16$
6	13	13	$[4.2 \pm 1.2]$	$[3.6 \pm 1.0]$	$2.78 \pm 0.25$	$0.463 \pm 0.042$
7	2	2	$[2.6 \pm 1.8]$	$[2.2 \pm 1.6]$	$2.34 \pm 0.23$	$0.0981 \pm 0.0097$
8	2	2	$[10 \pm 7]$	...	$3.03 \pm 0.30$	$0.0319 \pm 0.0032$
9	1	1	...	...	$3.65 \pm 0.33$	$0.0096 \pm 0.0009$

<sup>a</sup>Although this entry for  $LF_5$  has a smaller statistical error than that for  $LF_3$ , it is partly affected by the depth limit of  $BW_5$  at  $M_V \simeq 4.2$ .



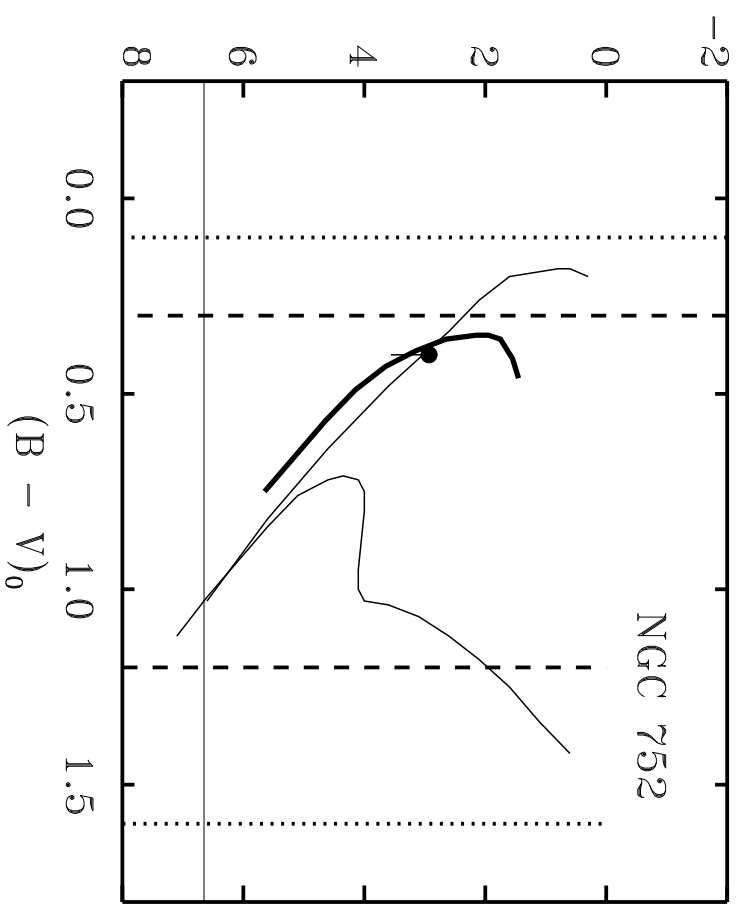
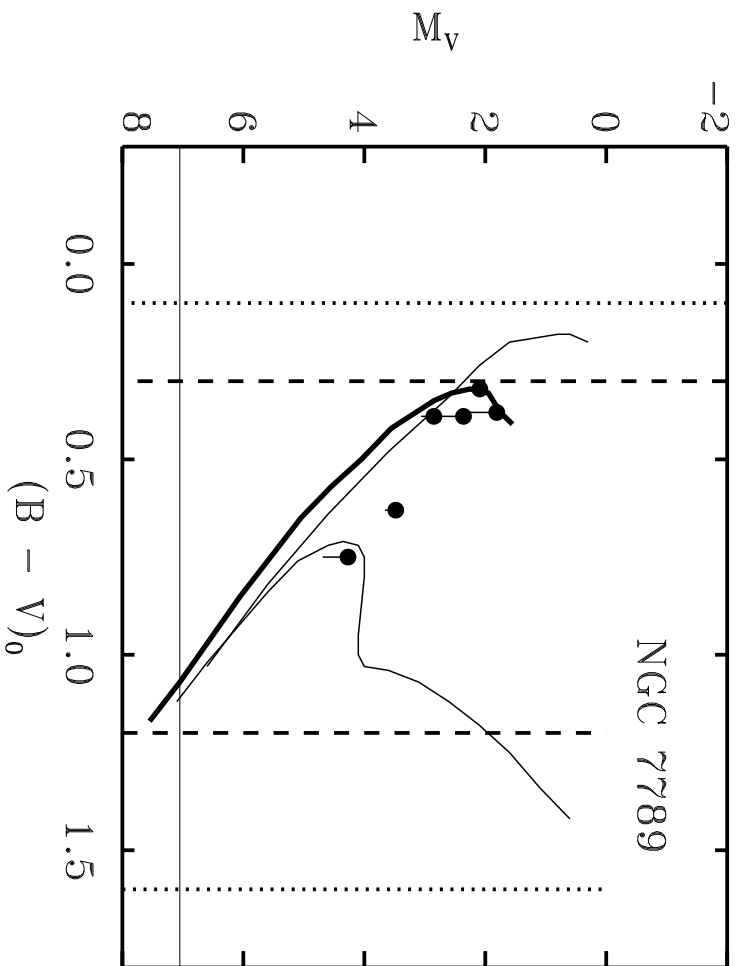
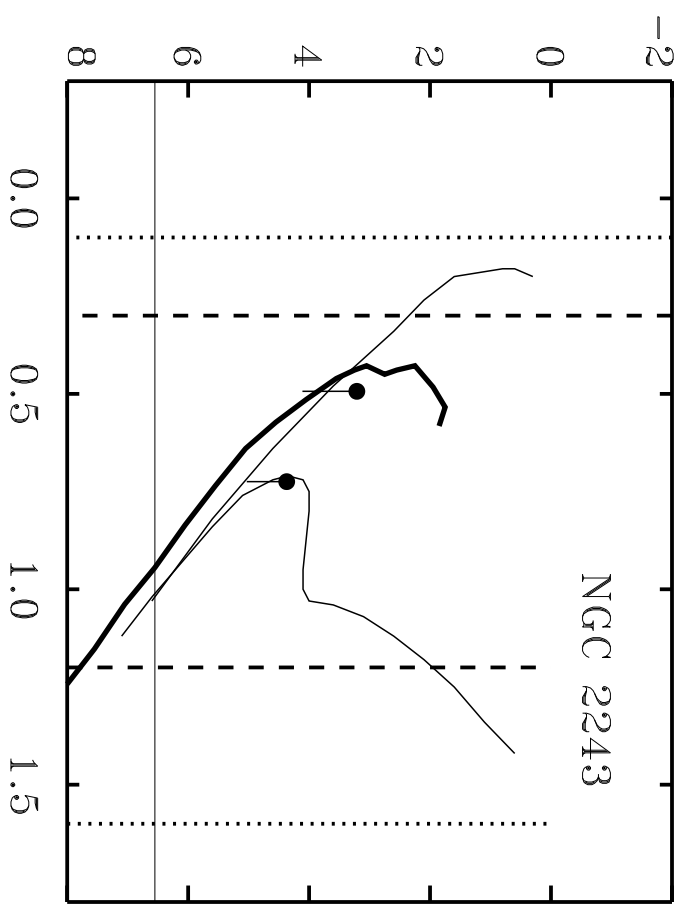
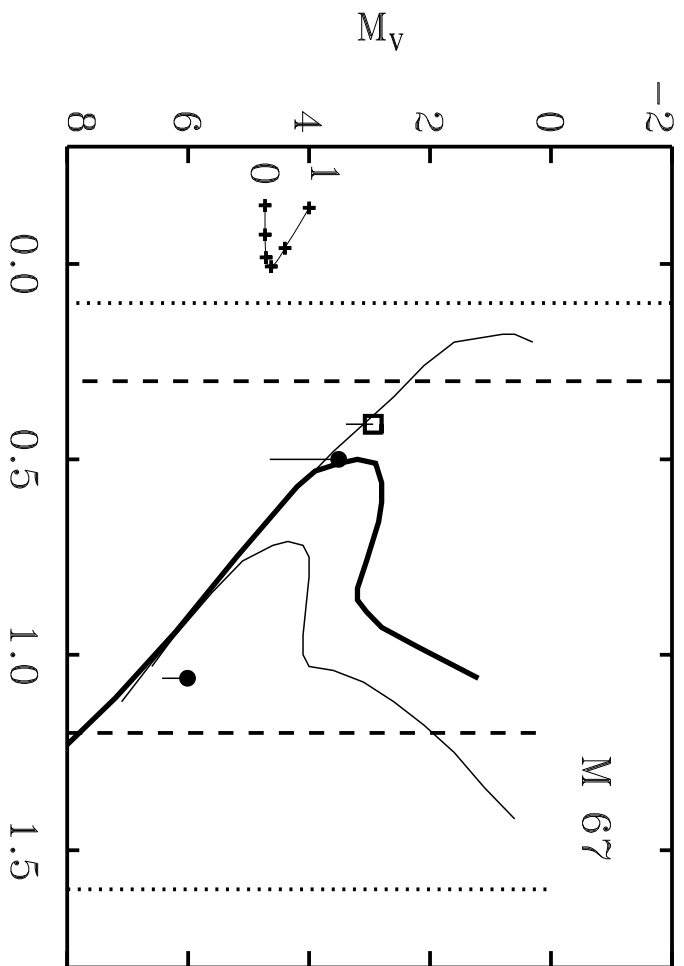


TABLE 6. Luminosity functions  $\text{LF}_{BW}^{corr}$  corrected for the galactic disk structure

$M_V$	$\text{LF}_3^{corr}$ ( $10^{-5}\text{pc}^{-3}$ )				$\text{LF}_5^{corr}$ ( $10^{-5}\text{pc}^{-3}$ )			
	$h_R = 2.5 \text{ kpc}$		$h_R = 3.5 \text{ kpc}$		$h_R = 2.5 \text{ kpc}$		$h_R = 3.5 \text{ kpc}$	
1	0.17 ±	0.17	0.21 ±	0.21	0.06 ±	0.06	0.09 ±	0.09
2	0.67 ±	0.34	0.85 ±	0.42	1.14 ±	0.27	1.65 ±	0.39
3	1.32 ±	0.34	1.69 ±	0.44	0.92 ±	0.14	1.40 ±	0.22
4	1.69 ±	0.32	2.19 ±	0.41	1.24 ±	0.12	1.91 ±	0.19
5	1.62 ±	0.29	2.10 ±	0.37	1.87 ±	0.26	2.91 ±	0.40
6	2.58 ±	0.72	3.36 ±	0.93	1.75 ±	0.49	2.73 ±	0.76
7	1.58 ±	1.12	2.05 ±	1.45	1.06 ±	0.76	1.65 ±	1.18

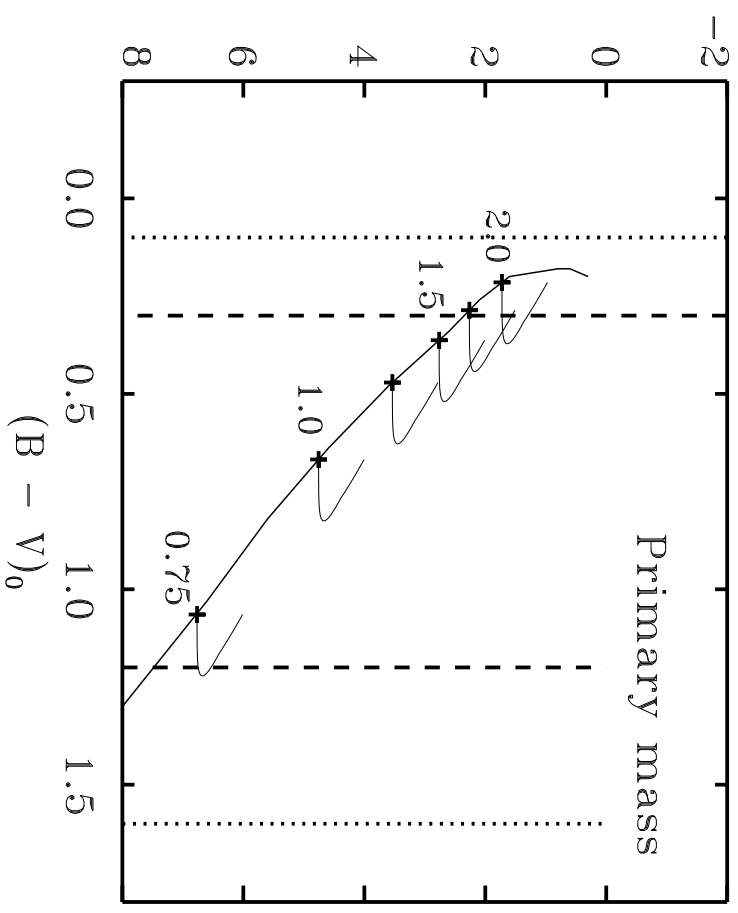
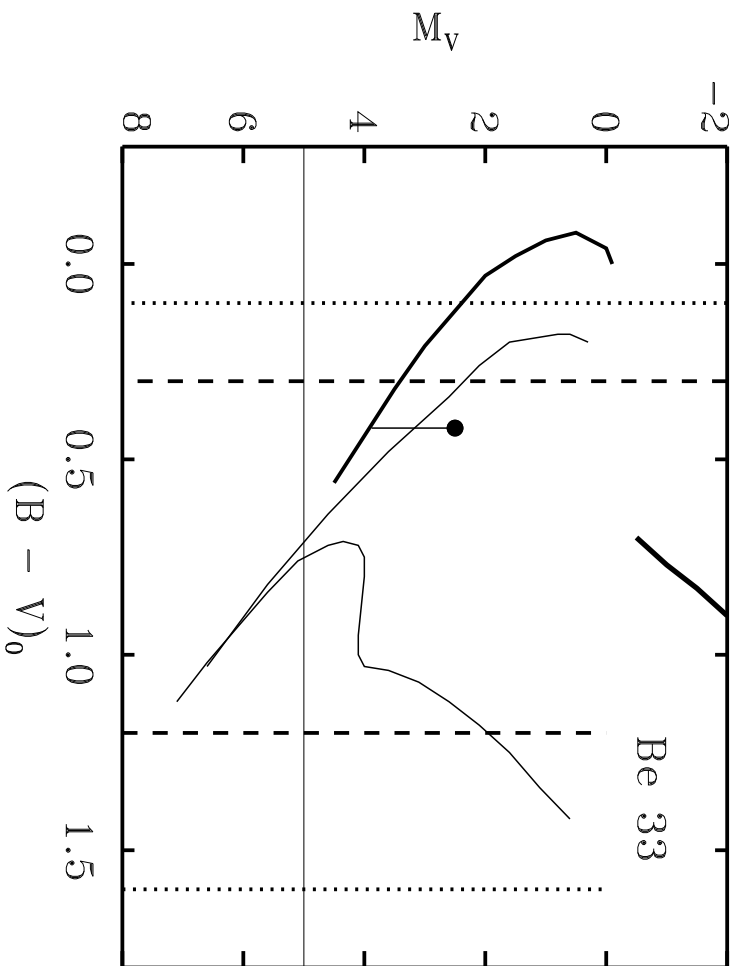
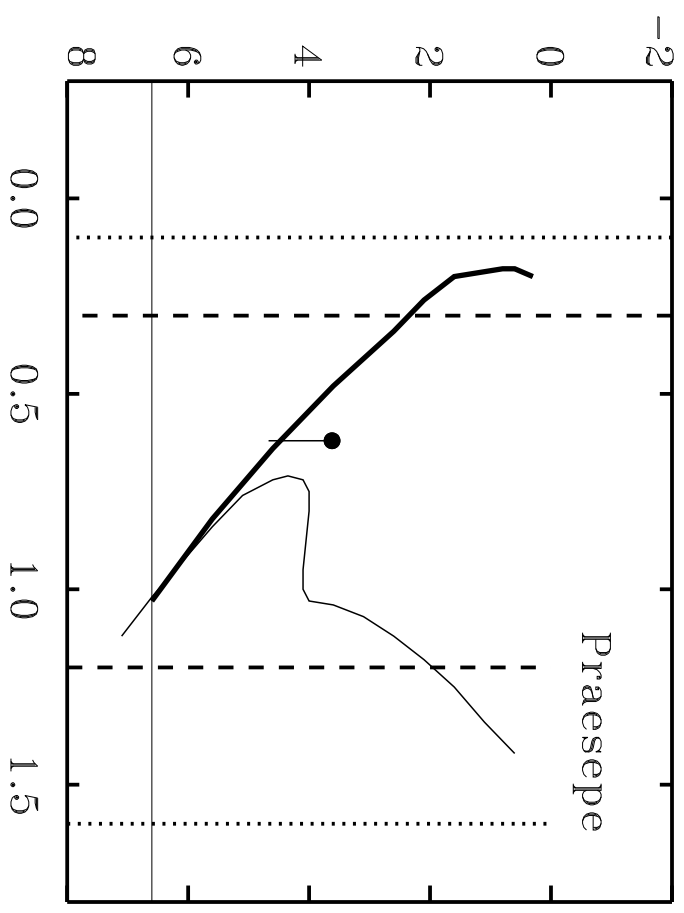
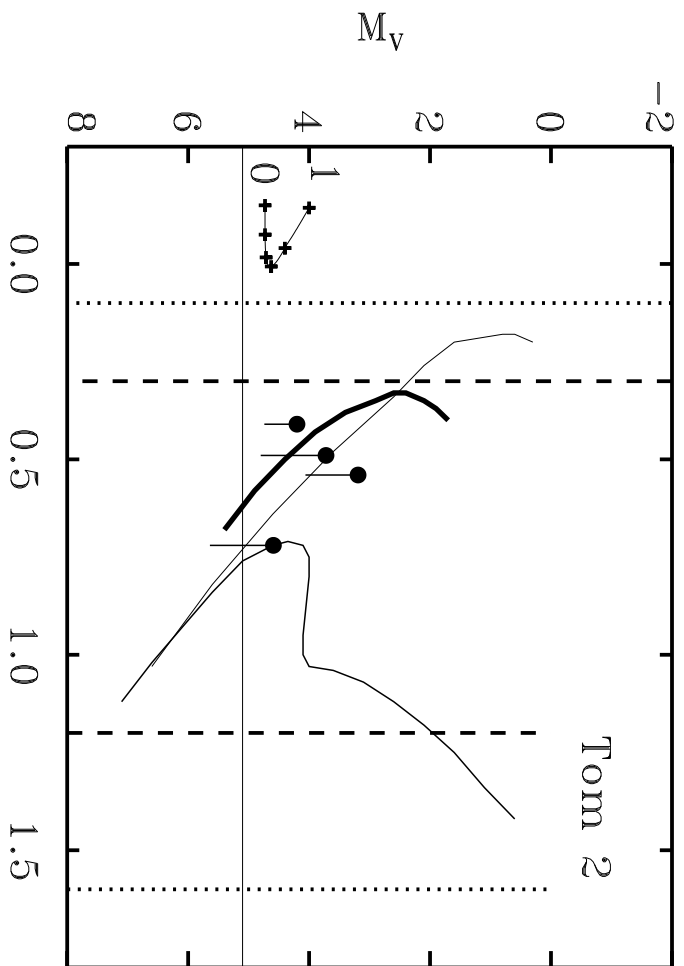


TABLE 7. Inverse frequency of occurrence of contact binaries ( $1/f$ )

$M_V$	BW <sub>3</sub>				BW <sub>5</sub>			
	$h_R = 2.5$ kpc		$h_R = 3.5$ kpc		$h_R = 2.5$ kpc		$h_R = 3.5$ kpc	
1	260 ±	260	200 ±	200	650 ±	650	450 ±	450
2	107 ±	57	84 ±	45	63 ±	20	43 ±	14
3	98 ±	29	76 ±	23	139 ±	30	92 ±	20
4	138 ±	30	106 ±	23	188 ±	28	122 ±	18
5	199 ±	40	153 ±	31	172 ±	29	111 ±	18
6	140 ±	41	108 ±	31	206 ±	60	132 ±	39
7	193 ±	138	148 ±	106	286 ±	207	184 ±	133
WM	134 ±	16	104 ±	12	128 ±	12	86 ±	8

